universität wien

MASTERARBEIT / MASTER'S THESIS

Titel der Masterarbeit / Title of the Master's Thesis

„Tristetraprolin beyond cytokine mRNA decay“

verfasst von / submitted by

Nora Elaine Bischoff, BSc

angestrebter akademischer Grad / in partial fulfilment of the requirements for the degree of

Master of Science (MSc)

Wien, 2020 / Vienna, 2020

Studienkennzahl lt. Studienblatt / degree programme code as it appears on the student record sheet:	A 066 830
Studienrichtung lt. Studienblatt / degree programme as it appears on the student record sheet:	Masterstudium Molekulare Mikrobiologie, Mikrobielle Ökologie und Immunbiologie
Betreut von / Supervisor:	Univ. – Prof. Mag. Dr. Pavel Kovarik

Acknowledgements

My gratitude goes to Prof. Pavel Kovarik for offering me a position in his lab, thereby allowing me to work in exactly the area of research that I am most interested in. Thank you for your support and your trust in me!

A lot of credit has to go to Martina Borroni for patiently introducing me to almost all techniques in the lab. Her extensive knowledge about the topic and her help during experiments and while writing this thesis, into which I was allowed to integrate a lot of her data, were indispensable for me. I could not have found a kinder and more generous supervisor – my sincerest thanks, Martina!

Working for my Master often didn't feel like work, mainly due to the wonderful people that I spent many an evening with and who are so open, supportive and funny that I feel incredibly lucky to know them. Thank you and you are great Flo, Annika, Kevin, Anita, Lidia, Lucy, Luisa and Fabian!

Content

1 Abstract

Tight regulation of the immune system's response to pathogens is vitally important for the health and survival of the host. Contributing to the resolution of inflammation and the re-establishment of immune homeostasis is tristetraprolin (TTP), which is often only seen as cytokine and chemokine mRNA destabilizing factor.

Previous work provided the interesting finding that mice lacking myeloid TTP survived *Streptococcus pneumoniae* infections better while also displaying reduced inflammation. To assess the role of TTP in this infection model, we investigated two different hypotheses. On the one hand, increased survival could be due to higher tolerance to pathogen-caused tissue damage. In this context, Amphiregulin (Areg), an EGF receptor ligand associated with cell differentiation, proliferation and wound healing, was examined as a potential TTP target. A reporter construct containing the 3'UTR of *Areg* downstream of a luciferase gene was used; however, mRNA stability assays and immunoprecipitation experiments failed to show definite TTP binding to Areg mRNA, probably due to technical issues.

On the other hand, improved resistance to the pathogen could explain the observed phenotype. Therefore, phagocytosis of different bacteria and latex beads was investigated in multiple macrophage types, showing that TTP limits particle uptake by macrophages. While the killing of ingested bacteria seems not to be affected by TTP, the increased phagocytosis of bacteria plays a role in a more successful response to bacterial infection in mice lacking myeloid TTP.

This study broadens the view on TTP and establishes the protein as an anti-inflammatory factor which is also involved in phagocytosis.

2 Introduction

2.1 mRNA stability

Gene product levels must be tightly controlled in any organism to ensure the smooth steering of a cell through the manifold challenges of its environment. Regulation can set in at any step, be it before or after transcription or post translationally on the protein level. Often there might even be multiple layers of regulation for a given gene. An especially fast way to control the output of a gene is to change the stability of the transcript, as product levels are decreased almost immediately even before a transcription stop could have any effect. This also prevents any waste of valuable material on protein production. Naturally, the reverse effect – increased mRNA levels due to higher stability – is also feasible. Changes in expression of a single gene regulating mRNA stability can influence multiple targets.

mRNA decay for quantity control has to be separated from mRNA decay for quality control, which includes nonsense-mediated decay of mRNAs with a premature stop codon as well as degradation of transcripts stuck on the ribosome because they lack a stop codon or because translation has been stalled. I will not discuss these mechanisms here. Furthermore, though many principles are similar in prokaryotic and eukaryotic cells, the focus shall only lie on mRNA stability and degradation in mammalian cells.

I will also just touch upon RNA interference (RNAi) here. In RNAi, microRNA (miRNA) or small interfering RNA (siRNA) guide the endonuclease Ago in the RNA-induced silencing complex (RISC), which cleaves the target leading to its degradation.[1] siRNA targets complementary RNA strands for degradation,[2] while partially complementary miRNAs in animals generally only repress translation.[3] It is evident that the protection of the genome from viruses and transposons is one of the main roles of RNAi, but it also acts to control expression of endogenous genes, most notably during development.[4] In this process, endonucleolytic cleavage, which is becoming increasingly more recognized as crucial step in determining mRNA stability, plays a major role.

Despite the diversity of mechanisms regulating mRNA decay, the process still relies on exonuclease activity and classically unfolds as follows: the poly(A) tail at the 3’ end is usually bound by poly(A)-binding protein (PABP) which protects the mRNA from degradation[5] and circularizes mRNA by interacting with eIF4G, aiding translation.[6] The stretch of adenine bases is shortened by deadenylases such as Ccr4-Caf1[7], Pan2/3[8] and poly(A)-specific ribonuclease (PARN) (in a 5’ cap (m7GpppN, where m is a methyl group and N is any nucleotide) dependent manner).[9] Following the removal of the 5’ cap by Dcp2[10], exonuclease decay is catalysed by Xrn1[11] in 5’-3’ direction and by components of the exosome from the 3’ end[12] (Fig. 1).

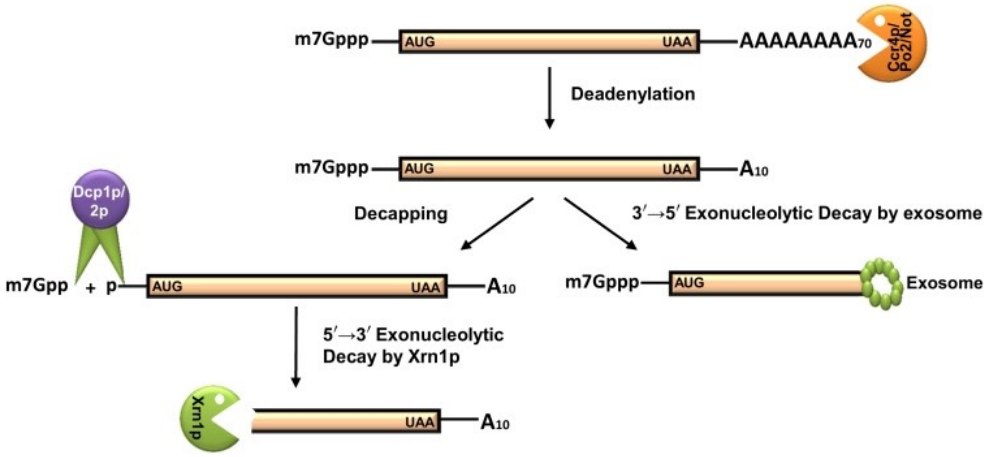

Fig. 1 General mechanism of mRNA decay Poly(A) tail at 3' end is degraded by deadenylases, the m7Gppp cap at the 5' end is removed by Dcp1/2 and exonucleolytic decay starting from both ends is carried out by Xrn1 and the exosome (from Das et et al., 2017[13])

2.2 Cis- and trans-acting determinants of mRNA stability

Specific mRNA sequences such as the poly(A) tail and AU rich regions in the 3' untranslated region (UTR) or secondary structures like 3' terminal stem loops in histone mRNA are called cis-acting determinants of mRNA stability because they only influence the mRNA they are a part of. Trans-acting factors on the other hand are mostly mRNA-binding proteins that bind to cis elements and thereby influence mRNA decay. The same protein can act on many different mRNAs and in turn interact with multiple other factors to control their function. They depend on the state of the cell and the different signals it receives.

2.3 Sequences determining mRNA stability in the 3' UTR

Contrary to 3' UTRs, 5' UTRs don't directly regulate mRNA stability, but they rather influence translational efficiency, which in turn affects mRNA half-life. In particular, the cap structure comes to mind, which greatly affects translation – not surprisingly, mRNAs without cap structure are far less stable[14,15]. Additionally, introducing a stem loop into the 5' UTR also reduces mRNA half-life significantly by hindering translation.[16] Still, most factors known to affect mRNA degradation are part of or target the 3' UTR, including the already mentioned poly(A) tail.

2.3.1 GU-rich elements

Another sequence element in the 3' UTR are GU-rich elements (GUEs). Genome-wide analysis found that GUEs are present in at least 5% of human genes, which are mostly involved in nucleic acid metabolism, transcription, neurogenesis and developmental processes.[17] The 11-mer sequence UGUUUGUUUGU is enriched in the 3' UTR of short-lived mRNAs[18] but GUEs have a lower ability to destabilize mRNAs compared to AREs (which are discussed in the following), even though they follow

a comparable patterning in their sequence distribution and have a very similar core pentamer (GUUUG).[17] GUEs are bound by CUG-binding protein 1 (CUGBP1, also called CUGBP and embryonically lethal abnormal vision-type RNA binding protein 3-like factors 1 (CELF1)).[18] CUGBP1 has been implicated in splicing reactions,[19] but it also recruits PARN deadenylase and thereby initiates mRNA decay.[20] As such, CUGBP1 appears to be responsible for the tumour necrosis factor alpha (*TNF*) mRNA destabilization in C2C12 cells, but only when they are unstimulated, that is when TNFα expression is not induced. A stabilization requires disruption of CUGBP1 binding.[21]

In RNA-immunoprecipitation sequencing studies it was found that binding peaks of another mRNA binding protein, tristetraprolin (TTP), as well as hnRNPA2/B1 binding site UAGG often overlapped with CUGBP1 binding sites in introns and 3' UTRs. hnRNPA2/B1, a known splicing factor affecting alternative polyadenylation, for example binds to the telomeric repeat sequence UUAGGG which incidentally was enriched in TTP peaks. This could suggest that TTP interacts with CUGBP1 and hnRNPA2/B1 to regulate RNA stability and processing, but as these results were generated in TTP overexpression experiments in HeLA cells, they have to be viewed with extreme caution.[22] These findings have yet to be validated in a less artificial system and should be handled as speculation.

2.3.2 **AU-rich elements**

Most studied are probably AU-rich elements (AREs). It is estimated that 58% of human protein coding genes contain AREs in introns and 20% contain them in 3' UTRs.[23] Chimeric RNAs of normally stable transcripts with added AREs are rapidly degraded, as shown in first experiments with the β-globin mRNA which was fused to AREs derived from the granulocyte-macrophage colony stimulating factor (*GM-CSF*) gene.[24] However, these sequences can increase or decrease mRNA half-life depending on which proteins bind, which might in part depend on the kind of ARE. These have been classified into three types: Class I which contains 1-3 AUUUA elements in the vicinity of a U-rich region, class II which has at least two overlapping UUAUUUA(U/A)(U/A) elements in a U-rich region, and class III which lacks AUUUA pentamers but contains U-rich regions.[25] Although this classification is not based on biological function, it has been noticed that most of the mRNAs that contain class II AREs code for cytokines while mRNAs encoding other proteins such as transcription factors often contain class I and sometimes class III AREs.[26] It should be noted that this classification is arbitrary and that all these different elements might have similar functions in cells. Many ARE binding proteins have been identified, some of which I will list here.

2.4 **ARE-binding proteins**

2.4.1 **AUF1/hnRNPD**

ARE/poly(U)-binding factor 1 (AUF1), also called heterogeneous nuclear ribonucleoprotein D (hnRNPD), was the first ARE binding protein that was isolated.[27] It shuttles between cytoplasm and nucleus (which affects mRNA degradation rates)[28] and binds to both class I and II AREs[26] but has a bigger stabilizing effect on class II AREs. AUF1 seems to change the mRNA's structure once it is bound to ARE and might therefore offer binding possibilities for other interaction partners, e.g. allowing access to deadenylases.[29] AUF1 competes with PABP for poly(A) binding[30] and can recruit the exosome to the mRNA.[31] It has a dual role in mRNA stability and this effect might be cell type dependent as it destabilizes mRNA in K562 pro-erythroblast cells[32] and stabilizes it in NIH-3T3 fibroblast cells.[33] Additionally, while AUF1 was first shown to promote degradation of Myc mRNA[32], it can also protect it in proliferating cells with high levels of AUF1 such as fetal hepatocytes.[34]

These opposite roles could be the result of alternative splicing of the AUF1 mRNA, which creates four isoforms of the protein whose expression patterns and functions may differ. Their binding affinity and stabilizing effect decrease in this order: p37 ≥ p42 > p45 ≥ p40. All isoforms can block the RNA decay directed by the c-*fos* protein-coding region, a sequence motif totally different from AREs, in equal measure, but p37 and p42 (which both don't contain exon 2) are far better able to inhibit ARE-mediated decay.[33] The most abundant isoform p40 (containing exon 2) seems to be mostly responsible for destabilizing ARE containing mRNAs, since only selectively downregulating isoforms p45 and p40 (and not p45 and p42) increases the stability of an ARE-GFP construct and GM-CSF mRNA. This could be because p40 can be ubiquitinated and thus targeted for proteosomal degradation, which also leads to a decay of mRNA. p40 shares this property – corresponding to the lack of exon 7 – with p37, which nevertheless rather seems to be a stability promoting factor. Raineri et al. suggest that p37 and p42 gain access to ARE sequences once p40 levels are decreased, stabilizing the transcript. Furthermore they propose that the ratio rather than the absolute amounts of AUF1 proteins determine mRNA stability.[35] The complex interplay between isoforms in different cell types is far from resolved, as p37 has also been shown to enhance mRNA decay.[36] To complicated things, posttranscriptional modifications such as phosphorylation influence isomer binding and function as well.[37] For example, p38 mitogen activated protein kinase (MAPK) decreases AUF1 interaction with mRNAs[38] and downstream signalling of p38 has been shown to cause proteasomal degradation of AUF1.[39]

Table 1 Isoforms of AUF1

Isoform	Exon 2	Exon 7
p37	-	-
p40	+	-
p42	-	+
p45	+	+

Another mechanism of control is the direct binding of exon 7-containing isoforms AUF1p45 and p42 (but not p40 or p37) to the tandem zinc finger domain of TTP, whereby p45 improves TTP binding to ARE sites, while AUF1 itself is then not directly binding to RNA. AUF1 can thus contribute to or control TTP's mRNA degrading effect.[40]

2.4.2 **HuR/ELAVL1**

Human antigen R (HuR) or ELAV-like protein 1 (ELAVL1), the most prominent member of the Hu family, can also shuttle between the nucleus (where it is predominantly found) and the cytoplasm and is counted to the stabilizing ARE binding factors.[41] Out of all ARE binding proteins HuR is the one with the most binding sites in introns (in HEK cells in 5752 genes,[23] while another study in HeLa cells found only 2490 genes[42]). This suggests a role of HuR in splicing events and indeed sequestration of HuR by ARE-containing viral RNAs shows changes in alternative splicing and polyadenylation of cell transcripts.[43] This is particularly important in HuR's involvement in the germinal centre reaction and the whole B cell antibody response.[44] Moreover, HuR autoregulates its abundance in a negative feedback loop by binding to a GU rich element, which contains multiple copies of HuR's preferred motif (UUUAUUU), next to the primary poly(A) signal and thereby blocking it. This creates a longer transcript with a destabilizing ARE.[45] Another specific example would be alternative splicing of Tra2β mRNA in human colon cells under oxidative stress.[46]

Upon phosphorylation due to stress or growth factors, HuR binds mRNA in the nucleus and then both translocate to the cytoplasm.[47] The protein is phosphorylated among others by p38 kinases downstream of $G_{\alpha q}$-coupled G-protein coupled receptors which has been shown in the context of cardiomyocyte hypertrophy.[48] p38 activation results in the cytoplasmic accumulation of HuR and subsequent stabilization of survival motor neuron (SMN) mRNA.[49] Stabilizing ARE-containing mRNAs is HuR's most prominent role, in which it acts as an antagonist to TTP – in many cases competing with TTP for binding on the target. The proteins' opposing functions are also illustrated by knock-out studies showing that autoimmunity is promoted by TTP deletion, whereas it is reduced by HuR knock-out.[50] This is due to the fact that autoimmunity is dependent on immune cell activation which is promoted factors such as GM-CSF,[51] TNFα[52] and IL-2[53] whose mRNAs can either be stabilized by HuR or destabilized by TTP. Efficient *TNF* translation requires HuR binding and TTP inactivation by p38/MK2 phosphorylation, which reduces its ability to replace HuR and destabilize TNF mRNA.[54] Also, HuR promotes cell proliferation by stabilizing mRNA coding for cyclin A and cyclin B1[55] and is often overexpressed in cancer cells such as glioma cells, where it results in fast cell growth,[56] while it is decreased in senescent and quiescent cells.[57] In contrast, TTP has been shown to inhibit proliferation in many cancers'.[58,59] HuR's mRNA stabilizing role often relies on its binding close to miRNA binding sites and thereby preventing miRNA mediated decay. In such a way it stabilizes TTP mRNA by

antagonizing miR-27-mediated degradation.[60] On the other hand, HuR was also shown to promote degradation in a miRNA-dependent manner, as both HuR and miRNA let-7 were required for Myc mRNA degradation.[61] This contrasts HuR's previously described TTP-antagonistic role, which is also called into question by a study showing how HuR overexpression can reduce inflammation due to translational silencing of specific cytokines in macrophages.[62] All this suggests that HuR acts in a highly cell-type-, gene- and situation-dependent manner and that findings regarding its functions can hardly be generalized.

2.4.3 **KSRP**

K-homology/KH-type splicing regulatory protein (KSRP) is mostly involved in pre-mRNA splicing and miRNA maturation.[63] Nevertheless, there is also evidence that it is involved in ARE mediated mRNA degradation, decreasing the stability of IL-8, IL-6, Cox2 and Cxcl2/3 mRNAs in HeLa cells[64] and *TNF* and *Il1b* in astrocytes.[65] It has been shown to recruit the exosome and poly(A) ribonuclease (PARN) via its KH motifs.[66] KSRP knock-out increases the proliferation of CD4+ but not of CD8+ T cells and leads to higher levels of secreted cytokines upon stimulation.[67] Increased resistance to viral infection most likely stems from these higher IL-1 levels.[68] KSRP loss also skews the expression patterns in the direction of Th2 responses, likely due to increased stability of *Il4*.[67] More evidence for its contribution to cell fate determination comes from its involvement in granulopoiesis, where it indirectly (via miR-129) blocks Runt Related Transcription Factor 1 (RUNX1) synthesis[69], a transcription factor essential for normal hematopoietic development, especially granulocytic differentiation.[70] Not only has KSRP been linked to the control of immune responses but also to lipid metabolism, tissue regeneration, and the DNA damage response.[63] It furthermore interacts with TTP and HuR to regulate the stability of mRNAs such as *iNOS*[71] and seems to be regulated in a similar way as TTP, as phosphorylation by p38-activated kinases weakens KSRP binding to AREs and stops their rapid decay.[72]

2.4.4 **TTP**

Tristetraprolin (TTP) (named for the three repeats of four consecutive prolines) encoded by the gene *Zfp36* was also historically known as ZFP36, because it is a CCCH tandem zinc finger protein. Its eight cysteines and histidines in the tandem zinc finger domain are so important that a single mutation of one of them completely stops RNA binding.[73] Its optimal binding sequence is UUAUUUAUU. TTP belongs to a protein family including: TTP, ZFP36L1 (also known as cMG1, BRF1, ERF1, and TIS11b) and ZFP36L2 (also known as TIS11D, BRF2, ERF2) with rodents expressing also ZFP36L3.[74] TTP is predominantly found in the cytoplasm,[75] where it directly destabilizes many mRNAs, including its own. So far, only targets containing class II AREs have been identified.[26] Destabilizing activity is mostly limited to ARE binding in the 3' UTR, but around two thirds of 498 genes containing TTP binding sites found in LPS stimulated bone marrow derived macrophages (BMDMs) are positioned in introns. The

function of TTP at introns remains elusive, as it was shown that it does not destabilize mRNA and most likely also doesn't contribute to splicing.[76] It is also unclear how 70% of mRNAs containing an AREs in the 3'UTR are stable and 15% are unstable independently from TTP, when TTP promotes ARE mediated mRNA decay.[76] The fact that stable transcripts are often bound to TTP to a similar extend as unstable ones leads to the conclusion that TTP might not be sufficient for mRNA degradation. Examples for this are provided by interaction between TTP and miR16 to destabilize *TNF* mRNA in HeLa cells[77] and interaction between TTP and hnRNP F for destabilization of a subset of ARE mRNAs.[78] Moreover, TTP has been shown to decrease the stability of MHC Class I transcripts in dendritic cells, even though they do not contain AREs but another conserved sequence motif. Binding of another trans-factor to the motif which then recruits TTP could be an explanation, but the actual mechanism remains unknown.[79] TTP could of course also regulate mRNA levels indirectly, a potential example being *RelB*, which was found to be upregulated by TTP binding to intronic and exonic sites in its mRNA. Many TTP upregulated genes without TTP binding site contain RelB binding sites in their promoter. Interestingly, most of these code for genes that are required for type I interferon production and the innate anti-viral response.[22] This was only seen in HeLa cells overexpressing TTP and the results cannot be taken at face value. Moreover, TTP has been shown to rather downregulate the type I interferon response for example by directly targeting *IFNb*.[80] Still it is very likely that TTP influences gene levels indirectly by targeting genes that regulate others in turn.

TTP does not only influence the stability of mRNAs, but also seems to directly hinder their translation (in cooperation with other proteins). When TTP is expressed, Cullin 4B (Cul4B, a scaffolding component of cullin RING finger ubiquitin ligases) acts to dampen the TTP mediated decay by promoting mRNA loading to polysomes. This was examined using TNF mRNA.[81] Studies show that in TTP knock-out macrophages, the protein levels of factors like TNFα and GM-CSF increase to a larger degree than their mRNA levels (5-fold compared to 2-fold increase in *TNF*), indicating that TTP can act on the level of translation.[82] An important interactor is RCK/p54, whose silencing also increases protein levels in relation to mRNA levels, showing RCK/p54 as a functional partner of TTP in enhancing TTP-mediated translational repression.[83] Apparently, TTP and RCK/p54 are part of a large protein complex containing multiple processing body factors like Dcp1/2, which are decapping the mRNA and thereby also hindering translation while promoting mRNA decay.[84]

TTP has often been described as a phosphoprotein owing to the many phosphorylation sites that have been found and which are responsible for the 33.6 kDa protein to appear on western blots as a ladder of bands between 40 and 55 kDa.[85] TTP has been shown to be phosphorylated by extracellular signal-regulated kinase (ERK), cJun N-terminal kinase (JNK) and p38 mitogen-activated protein kinase (MAPK).[86] A crucial role is played by the serines at positions 52 and 178 in murine TTP, as their

phosphorylation by p38 MAPK-activated kinase MK2 results in TTP's localization in the cytoplasm.[85] Also, they increase the stability of the protein which is otherwise quite unstable and ubiquitin-independently degraded by the proteasome.[87] Enhanced stability might be conferred by the subsequent binding of 14-3-3- proteins, which also protects TTP from dephosphorylation[88,89,90]. The resulting complexes are excluded from stress granules - which are formed in response to stress and are crucial sites for determining mRNA fate - and ARE-mediated mRNA decay is prevented.[91] Protein phosphatase 2A (PP2A) has been shown to counteract MK2 by dephosphorylating S52 and S178[92] and the unphosphorylated protein can then bind to mRNAs with a higher affinity.[93] Only when S52 and S178 are unphosphorylated, TTP can specifically recruit the Ccr4/Caf1/Not deadenylase complex.[94] This occurs through direct interaction between Not1 and the C-terminus of TTP.[95] TTP can also recruit decapping complex Dcp1/2, 5'-to-3' exonuclease Xrn1 and the 3'-to-5'exosome via its N-terminal domain.[96] Accordingly, when S52 and S178 are mutated to alanine and can't be phosphorylated, TTP is highly active and more unstable. However, even in this context PP2A can still increase TTP activity, suggesting the contribution of other phosphorylation sites to deadenylase recruitment.[94] In general, the different functions of specific TTP phosphorylations are far from resolved, even the two best studied phosphorylation sites at S52 and S178 have not yet given up all their mysteries.

2.5 Inflammatory regulation of and by TTP

Fine tuning of the immune response, especially the inflammatory response, is imperative for the organisms to stay healthy and survive infections. The time precision of the immune response can be illustrated by the half-life times of cytokines, that range from 5 to 30min (*TNF* half-life in plasma),[97] which is extremely short compared to the median mRNA half-life in mouse embryonic stem cells of 7.1h.[98] During the immune response even a relatively minor change can have potentially catastrophic consequences: effective host defence is anything but trivial and the immune system has to be carefully balanced on a narrow path between efficient destruction of pathogens and tissue homeostasis. A weak inflammatory response might not be able to control the infection, but too strong induction of cytokines and reactive oxygen species can harm tissues and even result in a septic shock. Resolution of inflammation is crucial, as prolonged inflammation can cause tissue damage, become chronic and induce autoimmunity. Considering the tight regulation required during the immune response, it's not surprising that all the above mentioned ARE binding proteins are implicated in cytokine regulation, sometimes working together on the regulation of a particular target such as *TNF*. TTP is involved to a very high degree, indeed its primary function seems to be immune regulation, decreasing the levels of pro-inflammatory factors in a negative feedback loop and thereby promoting inflammatory resolution.

As already mentioned, TTP often binds to AREs in the 3' UTR of cytokines. Prominent targets of TTP, which are stabilized when TTP is absent, include mRNAs coding for GM-CSF,[99] IL-10,[100] Cxcl2, IL-1α,[101]

IL-1β, TNF,[102] IL-2,[103] p65/NFκB[104] and NLRP3, part of the NLRP3 inflammasome which is a central regulator in inflammation.[105] TTP does not only owe its importance as immune manager to its targets, however, but also to its own regulation.

In unstimulated cells TTP is present in low amounts, but it's very quickly induced in response to environmental stress, growth factors, bacterial products, and inflammatory cytokines, but also by anti-inflammatory factors such as IL-10.[106] The promoter of TTP contains a Gamma interferon activation site (GAS) element, which is a binding site for STAT1 dimers that have been phosphorylated by JAK1/2 upon IFN-γ and IFN-β receptor binding. Interferon induced STAT1 signal must be accompanied by p38 MAPK stimulus to activate TTP transcription. Bacterial products such as LPS activate both signals and LPS and interferons together synergistically induce strong TTP expression.[107] p38 MAPK continues to play a role in TTP regulation as the p38 MAPK-activated kinase MK2 phosphorylates it immediately after translation, blocking its mRNA destabilizing function. As the levels of activated p38 decrease over time, so does TTP phosphorylation, which in turn slowly upregulates mRNA decay (for example of *IFNG*)[101] (Fig. 2). This provides a nice negative feedback loop that stops the inflammatory response after the initial stimulus has been cleared, but not all questions have been solved. For instance, it makes sense for TTP to bind more genes 6h after LPS stimulation than 3h after LPS stimulation and there is evidence that the transition to the resolution phase of inflammation later after the stimulus is a result of differential TTP binding. Some targets, like *TNF*, are destabilized throughout the inflammatory response, while others, like *Cxcl2*, only becomes sensitive to TTP mediated decay at a later time point.[101] But how is that, when the preferences for binding sites are unchanged?[76] It has been suggested that p38 activity is a determinant for mRNA sensitivity to TTP-mediated decay. *TNF* could be degraded at higher p38 activity, meaning lower TTP activity, while this could be insufficient for *Cxcl2*. Additional interactors could play a role too - TNF mRNA can even be degraded TTP independently, but this is inhibited by LPS stimulation and therefore can't explain differential decay sensitivities in this context.[101]

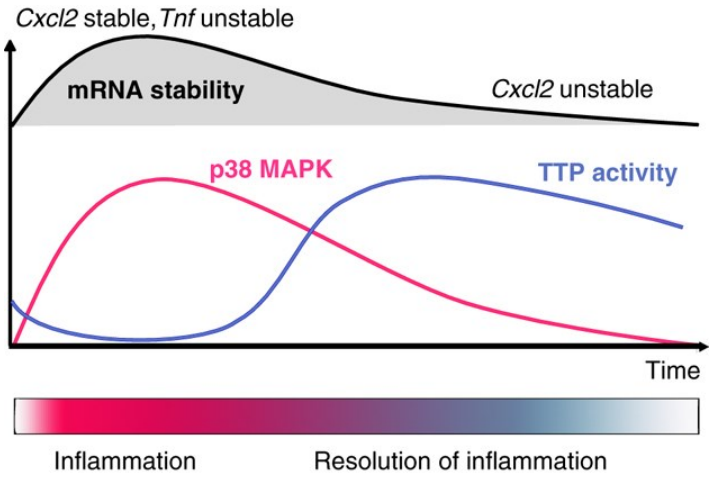

Fig. 2 TTP regulation in inflammation p38 MAPK activation at the onset of inflammation increases TTP expression but inhibits its activity which increases as p38 levels decrease. TTP then destabilizes many mRNA transcripts thereby promoting inflammatory resolution (from Kratochvill et al., 2011[101])

Another pathway for TTP induction starts with increased CD38 (NAD glycohydrolase (NADase)) levels at the onset of inflammation. CD38 synthesizes ADP ribose (ADPR), cyclic ADPR (cADPR) and nicotinic acid adenine dinucleotide phosphate (NAADP) from $NAD(P)^+$ which is released by damaged or stressed cells as a danger signal. cADPR and NAADP promote cytokine secretion by increasing intracellular Ca^{2+} levels but they also increase TTP expression via cAMP/PKA/CREB pathways at the start of inflammatory resolution which then decreases the levels of ARE containing *CD38*. This increases NAD+ levels inducing Sirt1, which deacetylates and thereby activates TTP that can then fully display its anti-inflammatory functions.[108]

Inhaled carbon monoxide has also been shown to induce TTP expression and enhance mRNA decay after lung injury using a similar pathway.[109] Carbon monoxide releasing molecule 2 (CORM2) increases levels of cAMP and NAD+, and phosphorylation of CREB via PKA. TTP expression is increased and the reason for CO activated promotion of inflammatory resolution.[108]

2.5.1 **Detrimental effects on health by TTP knock-out**

TTP's immunological role is strikingly seen in TTP knock-out mice which are born healthy but soon suffer from cachexia (muscle loss) and severe autoimmunity diseases such as alopecia, erosive arthritis, dermatitis, conjunctivitis, as well as increased production and tissue infiltration of neutrophils, lymphocytes and macrophages. They also express high levels of antinuclear antibodies targeting contents of the cell nucleus. As treatment with anti-TNFα antibody soon after birth prevented most of the symptoms, *TNF* was established as one of the most important if not the most important target of TTP.[82] A following paper showed that the half-life time of TNFα mRNA following LPS stimulation was increased from around 39 to approximately 85 minutes in TTP-deficient macrophages.[110] However, *TNF* is not the only TTP target responsible for the severe hyperinflammation observed in TTP knock-out mice, as demonstrated by the milder phenotype described in *Il23*$^{-/-}$ *Zfp36*$^{-/-}$ [111] and *Il1R*$^{-/-}$ *Zfp36*$^{-/-}$ mice.[112] The autoimmune phenotype is therefore clearly the result of changed levels of multiple cytokines and chemokines.

TTP is mostly studied in myeloid cells, especially neutrophils and macrophages, but TTP is also expressed in lymphocytes, fibroblasts and keratinocytes.[113] Myeloid specific TTP knock-out mice only exhibit a minimal phenotype compared to the full body knock-out mice described above. They develop normally except for a slightly reduced weight gain and a super-sensitivity to LPS showing that other cell types contribute significantly to the full knock-out phenotype.[114] Support for this comes from mice lacking TTP in keratinocytes: they exhibit a spontaneous "full body TTP KO-like" phenotype characterized by systemic inflammation, psoriatic-like skin lesions, and dactylitis, which also seems to be driven by TNFα.[113] This suggests that many symptoms of the full body TTP KO can be attributed to keratinocyte derived TNFα. However, when bone marrow from TTP knock-out mice was transplanted

to RAG2 deficient mice (which are unable to produce B and T lymphocytes), these mice recapitulated the full body TTP phenotype after a couple of months indicating that cells stemming from a hematopoietic progenitor must be responsible after all.[115] These were most likely no lymphocytes as systemic TNFα in response to LPS was mainly traced back to myeloid cells such as macrophages and neutrophils.[116] TTP-deficient macrophages were exposed to be major producers and accumulators of TNFα, again incriminating myeloid cells as responsible for the TTP knock-out phenotype.[115] There has been some evidence that keratinocytes can derive from the bone marrow and engraft in skin[117,118], but whether this really is the reason for the re-established phenotype seems unlikely and remains only a vague idea, even though it would explain why myeloid-specific TTP deficiency only results in such a limited phenotype compared to the full body TTP knock-out.

2.5.2 **Health promoting effects of TTP overexpression**

Strongly and constitutively overexpressing TTP leads to embryonic lethality,[119] but this problem can be bypassed by deleting the ARE in the 3' UTR of *Zfp36* which leads to increased TTP stability while still keeping its regulation intact. By using this system, effects of TTP overexpression could be studied in several models of inflammatory diseases. Overexpressed TTP almost completely protected mice from collagen antibody-induced arthritis, a widely used model of human rheumatoid arthritis. Besides, TTP overexpression reduced the levels of inflammatory proteins and neutrophil recruitment to the skin in a model of induced dermatitis that resembles psoriasis in humans. Furthermore, mice with more stable TTP were protected from weight loss and neurological dysfunction in a model of experimental autoimmune encephalomyelitis which resembles human multiple sclerosis.[120]

The phenotype observed upon TTP overexpression can be recapitulated in mice expressing a hyperactive form of TTP. TTP's activity was increased by creating a mutated version of the protein that contains alanine instead of serine residues at positions 52 and 178. The mutations abrogate TTP's phosphorylation at these sites and prevent inactivation of the protein (see above, *2.4.4 TTP*). Mice expressing this form of TTP exhibited a reduced inflammatory response to LPS due to increased mRNA degradation of pro-inflammatory cytokines.[89]

The quantity and activity of TTP are reduced in several cancers; and the absence of TTP in cancer cells enhances cancer progression and reduces survival. When TTP was instead overproduced in gastric cancer (GC) cells, it inhibited tumour growth by inhibiting IL-33[59] and programmed death-ligand 1 (PD-L1) which decreased infiltration of regulatory T cells (Tregs) and increased cytotoxicity against TTP-overexpressing GC cells.[121] Off note, IL-33 has been shown to increase the number of Amphiregulin producing ST2 (IL-33 receptor) Tregs and Areg promoted metastatic tumour growth in the lungs.[122] This shows a mechanism of IL-33 mediated cancer promotion and how it could be reduced by TTP (see also *2.6.1 Amphiregulin*).

2.5.3 **Health promoting effects of TTP knock-out**

TTP deletion from colonic epithelial cells in mice promoted intestinal barrier function and reduced susceptibility to dextran sodium sulphate-induced acute colitis. Part of these effects can be traced back to higher levels of inducible nitric oxide synthase (Nos2) in colonic epithelial cells, which is targeted by TTP. While increased Nos2 expression in macrophages enhanced colitis, it had the opposite effect in epithelial cells and one could assume that TTP plays equally diverging roles in these cell types.[123]

As mentioned above, myeloid specific TTP knock-out leads to severe endotoxic shock syndrome when mice are challenged with LPS, primarily owing to TNFα overexpression by macrophages and also dendritic cells[114, 124]. Very interesting consequences of myeloid specific TTP loss are reduced bacterial dissemination and increased survival rates of mice in response to soft tissue infection with *Streptococcus pyogenes*. Pathogen-engaged TTP-deficient neutrophils express higher levels of myeloid cell leukaemia 1 (Mcl1) (an antiapoptotic factor) due to higher mRNA stability and they display decreased apoptosis and more accumulation at infection sites. Although there is severe tissue damage at the site of infection due to hyperinflammation, the advantages to the host prevail.[125]

These results cannot be extrapolated to other infection systems though. While myeloid specific TTP deficiency also increases survival of intra-nasally infected mice with *Streptococcus pneumoniae*, this is not due to any changes in neutrophil behaviour, as neutrophil specific TTP knock-out didn't prolong life expectancy in mice. Contrary to infection with *S. pyogenes*, lack of myeloid TTP in this infection model reduces inflammation at the site of infection, but still inhibits bacterial growth and dissemination. While there is no change in immune cell abundances, TTP loss seems to affect cell activity, namely of alveolar macrophages which show increased phagocytic activity – at least in vitro.[126]

Besides showcasing the cost of negative immune regulation, these studies also provided more evidence of cell type specific roles of TTP, for example in macrophages and neutrophils. Clearly, macrophage and neutrophil transcriptomes are differently affected by TTP loss. Other examples for this are IL-6 only being limited by TTP in macrophages and Nos2 only limited in neutrophils.[125] TTP-mediated decay also differs between macrophages and dendritic cells. For instance, half-life of *Il1b* is affected by lack of TTP in bone marrow derived dendritic cells (BMDCs) but not in BMDMs.[127] All this shows the highly context dependent nature of TTP/ARE-mediated mRNA degradation.

It hasn't been shown yet whether TTP deletion in myeloid cells increases mice survival to bacterial infections by affecting resistance (ability to fight the pathogen), tolerance (ability to limit or repair tissue damage) or a combination of both (which is likely as so many mechanisms of the immune system rely on a complex interplay between different sometimes contrary processes).[128, 129]

2.6 **Tolerance mechanisms**

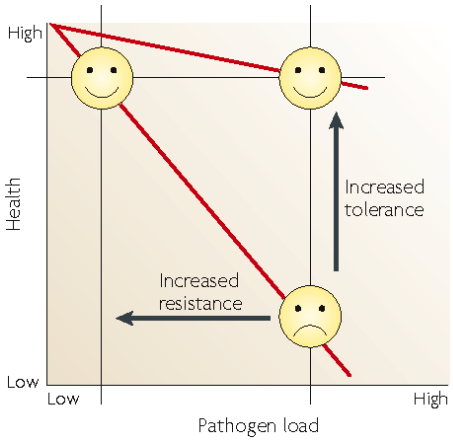

Fig. 3 Tolerance curve Health in relation to pathogen load can be affected by tolerance or resistance mechanisms, whereby a sign of the former is good health despite high pathogen load, and a sign of the latter is good health due to reduced pathogen numbers (from Schneider and Ayres, 2008[128])

While studying the fight against infection and potential therapies, resistance, which indicates the host's ability to reduce pathogen burden, has been the focus of attention. However, tolerance, which indicates the host's ability to endure pathogens, can be as important in controlling the pathology of infection. Mechanisms of tolerance haven't been extensively studied but Schneider and Ayres proposed a classification system of tolerance mechanisms in three groups that could make it easier to identify and examine them. To visualize the relationship between resistance and tolerance they introduced the tolerance curve which plots the pathogen load against the host's health (Fig. 3). The flatter the curve, the better the host's health compared to its pathogen load/the higher the host's tolerance against the pathogen. In the first class they group molecules that are classically viewed as mediators of resistance, but they argue can also be counted among the tolerance factors because they evolved to cause less harm to the host than invaders (e.g. antimicrobial peptides) or to only act against the foreign but not the self (Toll like receptors, antibodies). Looking at them in this way offers a different perspective on them. The second group is made up of effectors like TNF which act pro-inflammatory but not in a direct way. They seem to be considered a tolerance factor only because they affect the slope of the tolerance curve, although it rather increases the slope instead of decreasing it like a positive effector of tolerance would. Finally, the third group consists of factors that are clearly separated from resistance, such as detoxifying enzymes, factors preventing tissue damage or repairing it.[128]

Mouse strains have been shown to differ significantly in their ability to resist but also tolerate infections, and these two ways to deal with an attack on the host's health seem to be inversely correlated, indicating a trade-off between them.[130] Apparently, different mouse strains can control an infection by either being better at resisting or tolerating it. As such BALB/cAnN mice limit pathogen numbers, while they stay high in C57BL/6N mice which still don't develop severe arthritis in response to *Borrelia burgdorferi* infection.[131]

This trade-off ties back to the immune system's balance of pro- and anti-inflammatory signals, where the former can be counted to the resistance and the latter to the tolerance promoting factors. TTP as a balancing factor which counteracts pro-inflammatory cytokines and acts to downregulate the inflammatory response after the initial peak is part of the tolerance program. It also balances anti-

inflammatory responses. For example, it destabilizes *Il10* in a negative feedback loop for a return to an alert immunological state: TTP is induced by IL-10 by Stat3 recruitment to its promoter and a reduction of p38 kinase activity and can then contribute to the full anti-inflammatory response.[132, 133]

2.6.1 **Amphiregulin**

Transcriptome analysis in alveolar macrophages (AMs) revealed epiregulin and amphiregulin (Areg) among the factors that are differentially expressed upon TTP knock-out. These two factors have largely overlapping functions: they are low affinity ligands for the epithelial growth factor receptor (EGF-R) and they contain AREs which could be targeted by TTP. I will focus on Amphiregulin as its overexpression in absence of TTP has already been confirmed by quantitative PCR. [134]

Areg is first expressed as a transmembrane precursor and can then be cleaved by ADAM-17 at several alternative cleavage sites to be released from the cell.[135] In contrast to other EGF-R ligands, Amphiregulin binds with a very low affinity[136] to both EGF-R homodimers and EGF-R/ErbB2 heterodimers, inducing only half of the dimerization compared to high affinity ligands such as EGF, transforming growth factor alpha (TGFα), and betacellulin (BTC).[137] High affinity ligands induce rapid receptor internalization and degradation which together with re-stimulation produces an oscillating MAPK signal. Areg fails to do so, likely because it doesn't phosphorylate EGF-R as much as other ligands. Therefore, the signal doesn't abate but is stable instead.[138] Growth factor receptor-bound protein 2 (GRB2) recognizes phosphorylated receptors and recruits SOS and RAS which starts the RAF-MEK-ERK and PI3K–PDK–AKT signalling cascades, which regulate themselves by negative feedback loops.[139] Sustained activation of ERK has been found to induce differentiation while an oscillating signal seems to promote proliferation (in PC12 and other cells).[140] Areg can therefore induce differentiation across several cell lines such as PC12 cells,[141] kidney derived MDCK cells,[142] mammary epithelial cells[143] and myoepithelial cells,[144] while also inducing proliferation in others. The reasons for this are not yet clear. Fitting to those functions, Areg transcription has been shown to be driven by β-catenin signalling due to β-catenin-TCF responsive elements in its proximal promoter,[145] which it is also regulated by (probably tissue specific) transcription factors, such as HIF2α in myocardial tissue[146] or WT1 in kidney and liver.[147, 148]

Amphiregulin's proliferative effects contribute to tissue healing, but they are also crucial during normal development. Areg stimulates growth in epithelial mammary cells, fibroblasts, acts as a mitogen on hepatocytes to promote liver regeneration (where it is only expressed following injury) and is involved in physiological development of mammary glands, neuronal and bone tissue, and branching processes in prostate, kidneys and lungs.[148, 149] For these reasons, Areg has been identified to play a role in many

cancer types, for example contributing to independence from external growth signals, angiogenesis, metastasis and evasion of apoptosis.[149]

Areg promotes proliferation of keratinocytes and seems to be vital for their mitosis, as its absence leads to growth arrest, which could not be rescued by other EGF-R ligands or exogenous Areg.[150] Proliferation occurs via activation of the FoxM1 transcription factor, which has many binding sites in the promotors of mitosis relevant genes.[151] On a side note, FoxM1 is also highly expressed in lungs of patients suffering of idiopathic pulmonary fibrosis, where it has a pro-fibrotic function in epithelial cells and fibroblasts. Its deletion in macrophages, however, further increased fibrosis, indicating an anti-fibrotic activity. In macrophages, FoxM1 decreased p38 signalling, which seemed to contribute to fibrosis, and increased the p38 inhibitor Dusp1, while also taking part in collagen degrading activity.[152] Therefore, one could hypothesize that FoxM1 increases fibrosis in epithelial cells and fibroblast, while decreasing it in macrophages. Whether the same can be said about Amphiregulin still needs to be investigated.

Differentiation promoting function of Areg has also been associated with tissue repair. For instance, Areg causes the differentiation of tissue resident pericytes into myofibroblasts via TGF-β, which then produce collagen and promote wound healing by restoring the vascular barrier function.[153] Interestingly, Areg expression has also been shown to be increased by TGF-β and may be partly responsible for its growth inhibitory effects.[154] Furthermore, muscle injuries could heal better when injecting Areg into the damaged tissue where it can increase the differentiation of skeletal muscle satellite cells. In vivo, it is expressed by a specific form of muscle resident Tregs.[155] Areg also prevents tissue damage during LPS stimulated lung inflammation by inhibiting apoptosis of epithelial cells in a caspase 8 dependent manner.[156] Additionally, Areg promotes the restoration of the bronchial epithelium after lung infection with influenza virus where it is expressed by innate lymphoid cells (ILCs).[157]

Areg has also been shown to directly contribute to the resolution phase of inflammation by dissolving the accumulation of neutrophils and macrophages and reducing levels of TNFα, IL-6, and Cxcl1 in the lung after inflammation in response to agricultural dust exposure.[158] Moreover, Areg increases the secretion of exosomes containing immunosuppressive miRNAs from Tregs to effector T cells.[159] Mast cell derived Areg enhances Treg function in the tumour microenvironment, thus contributing to immune suppression and immune evasion of cancer cells.[160]

Notwithstanding its role in development, tolerance and resolution of inflammation seem to be the most important roles of Areg. Areg knock-out mice show only few abnormalities under normal conditions (mainly defects in mammary gland development)[161] but they are unable to resolve

inflammation upon an immunological challenge.[162] Apparently, other EGF-R ligands can compensate for or at least mitigate Areg loss in everything but tolerance to infections.

Although many epithelial and mesenchymal cell types express Areg, immune cells and particularly those associated with type 2 immunological responses are primary producers.[162] Type 2 responses are stimulated by multicellular pathogens and are associated with allergic responses and induction of T helper 2 cells secreting IL-5, IL-9, IL-10, IL-13 and IL-4, which promotes B cell responses and immunoglobulin E (IgE) expression. These pathways often overlap with those promoting tolerance, although the latter can be activated by a broader array of stimuli.[163, 164] Fittingly, T helper 2 cells are shown to express Areg which increases epithelial cell proliferation and shedding – a process employed to clear intestinal helminths. This is the only case known so far in which Areg not only acts as a factor conveying tolerance, but also resistance to an infection.[165]

The evidence showing Areg as a promoter of inflammatory tolerance taken together with the finding that Areg is overexpressed in TTP-deficient myeloid cells might in part explain the observations in *S. pneumoniae* infected mice. Increased levels of Areg could dampen inflammation at the infection site and Areg-induced tissue healing could contribute to increased survival. To date, its overexpression does not explain why bacterial growth and distribution are inhibited though. How far Areg can be implicated in TTP dependent control of infections remains to be seen. What is clear already, is that Amphiregulin is just a small piece in the puzzle that is TTP's contribution to pathogen specific immune responses.

2.7 Resistance mechanisms – phagocytosis

As discussed above, tolerance factors like Amphiregulin are not enough to effectively end an infection and they must be supported by active pathogen elimination. Many different cell types can perform phagocytosis, but it's mostly carried out by professional phagocytes like macrophages, neutrophils and dendritic cells. Phagocytosis does not only remove foreign particles but also apoptotic bodies and thereby contributes to tissue homeostasis. As this is not directly linked to the fight of infection however, I will not discuss it here.

Despite the importance of phagocytosis in the response to pathogens, its mechanisms haven't been characterized in detail yet. We know, however, the basic steps of this process: a particle or cell of at least 0.5µm is recognized by receptors on the phagocytic cell's surface, which trigger intracellular signalling leading to cytoskeletal rearrangements which culminate in particle internalization. Phagocytes can recognize foreign particles though different types of receptors, which activate different signalling pathways ultimately leading to the same outcome. Receptors such as Fc recognizing receptors bind to foreign particles via opsonins (antibodies and parts of the complement system) and downstream signalling is well characterized. After opsonin binding, the receptors cluster together and

are phosphorylated at their immunoreceptor tyrosine-based activation motifs (ITAM) by Src family kinases. Syk can bind and is phosphorylated, leading to the association of multiple adaptor proteins like LAT, Grb2 and Gab2, which associates with phosphatidylinositol-3,4,5-trisphosphate [$PI(3,4,5)P_3$]. Finally, small GTPases Cdc42, Rac1 and 2 and RhoA cause actin rearrangements which lead to the internalization of the particle[166].

Pattern recognition receptors (PRRs) on the other hand recognize pathogen associated molecular patterns (PAMPs) on foreign organisms. The response to their stimulation depends on the PRR activated and can either induce phagocytosis (for example through the mannose receptor), induce inflammatory signals through toll-like receptors (for example TLR4 after recognizing LPS[167]) or do both through scavenger receptors such as SR-A, CD36 or MARCO (macrophage receptor with collagenous structure)[168, 169]. Studies with inhibitors showed that signalling after scavenger receptor stimulation requires tyrosine kinases, protein kinase C, phosphoinositide 3-kinase and JNK and ERK pathways but not phospholipase C[170], which is required for phagocytosis following opsonized particles.[171] There it abruptly decreases the concentration of phosphatidylinositol-4,5-bisphosphate ($PI(4,5)P_2$) in the inner leaflet of the plasma membrane by hydrolysing it to inositol-3,4,5-trisphosphate and diacylglycerol (DAG) which in turn promotes phagocytosis[166].

The mechanisms underlying scavenger receptor-mediated phagocytosis are still unclear. As TTP mostly has anti-inflammatory functions, it could be involved in the negative regulation of phagocytosis at least when it concerns the uptake of bacteria. The situation would be different when considering the ingestion of apoptotic bodies, where a phagocytosis promoting role would better fit TTP's anti-inflammatory role. TTP's negative effect on phagocytosis could explain reduced bacterial load and spreading after lung infection in mice lacking myeloid TTP, however, this study is the first attempt at showing TTP's involvement in phagocytosis.

Once the pathogen is engulfed, the phagosome undergoes what is known as maturation which is indicated by continuous vesicle trafficking controlled by Rab GTPases. The phagosome membrane carries distinct markers depending on the state of the phagosome, whose contents change to be able to digest proteins, carbohydrates and lipids. Fusion with lysosomes promotes the acidification of the pathogen-degrading organelle and activates hydrolases brought by the lysosome. V-ATPases pump in protons and NADPH oxidase produces reactive oxygen species to help destroy the pathogen.[166] The whole process is highly controlled and TTP could play a role there. Binding sites for TTP have been found for SLC4A7, a bicarbonate transporter important for macrophage phagosome acidification[172], and possibly for NOX2, NADPH oxidase 2,[76] but not for any vesicle trafficking proteins.

3 Aims

Even though the regulation of immune responses has been extensively studied, its precise mechanisms remain elusive. One of the main challenges in their unravelling lies in the diversity of stimuli and in the heterogeneity of tissues involved in the immune response.

The aim of this study was to describe mechanisms of how TTP and TTP-mediated mRNA decay regulate responses to lung infection with *Streptococcus pneumoniae*. The specific aims were:

1) Determination of infection parameters in $TTP^{\Delta M}$ and $TTP^{fl/fl}$ mice such as bacterial load, immune cell infiltration, tissue destruction and cytokine production.
2) Testing whether the mRNA of the Areg gene is targeted by TTP for degradation. *Areg* encodes amphiregulin which is a tissue-protective growth factor that might regulate the barrier function of the lung epithelium during infection with *S. pneumoniae.*
3) Investigation whether and how TTP regulates phagocytosis of bacteria by macrophages.

4 Results

4.1 Preliminary research and infection parameters

4.1.1 Myeloid TTP decreases survival of *S. pneumoniae* infections

Tristetraprolin regulates immune homeostasis and response to immunological challenges in a cell type specific manner. Knocking out the protein in different subpopulations of cells can have drastically different effects on the health of mice and on how they respond to immune stimulation. In this project we focused on mice lacking TTP in the myeloid cell lineage ($TTP^{\Delta M}$), meaning in macrophages, neutrophils, monocytes and dendritic cells, and to a lesser degree on mice lacking TTP only in neutrophils ($TTP^{\Delta N}$). $TTP^{fl/f}$ mice, which contain *loxP* sites flanking *Zfp36* but no Cre recombinase, served as wild type controls.

In previous experiments performed in the lab, $TTP^{\Delta M}$ and $TTP^{fl/fl}$ mice were intra-nasally infected with live *Streptococcus pneumoniae,* a gram-positive pathogenic bacterium. While more than half of all $TTP^{fl/fl}$ mice died within 10 days post-infection, almost 90% $TTP^{\Delta M}$ survived this time period (Fig. 4A). Myeloid TTP therefore reduced the odds of mice to survive bacterial lung infection.

Experiments with $TTP^{\Delta N}$ mice suggested that TTP loss in neutrophils does not play a significant role in the prolonged life expectancy of infected mice, because there was no difference in their survival rates compared to $TTP^{fl/fl}$ littermates (Fig. 4B). This led to the hypothesis that rather than neutrophils, other myeloid cells, especially macrophages, might be responsible for the observed phenotype in $TTP^{\Delta M}$ mice. In other words, TTP in macrophages might deter the successful elimination of pathogens by limiting the mice's response to the infection, while TTP has no such effect in neutrophils.

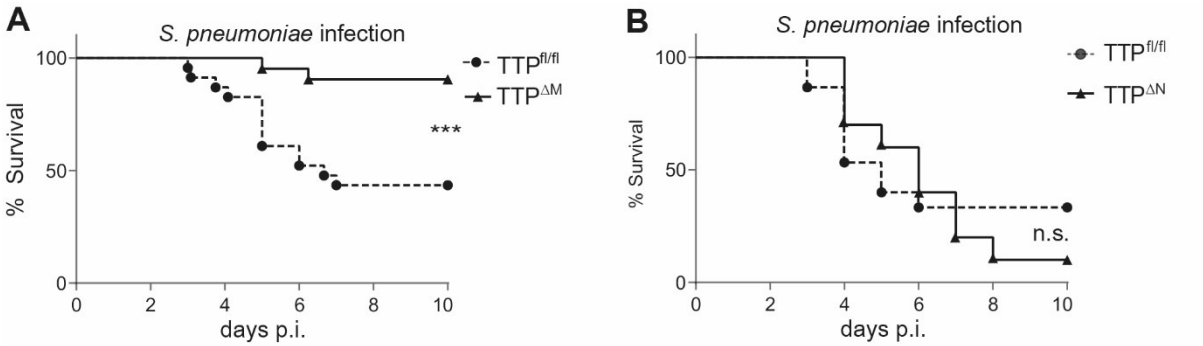

Fig. 4 TTP affects survival rates of mice Mice were infected with *Streptococcus pneumoniae* **A** Survival of $TTP^{\Delta M}$ and $TTP^{fl/fl}$ mice, n ($TTP^{fl/fl}$) = 20, n ($TTP^{\Delta M}$) = 23. **B** Survival of $TTP^{\Delta N}$ mice, n ($TTP^{fl/fl}$) = 14, n ($TTP^{\Delta N}$) = 10. Data generated by Maša Ivin.

4.1.2 Reduced local and systemic inflammation in TTP$^{\Delta M}$ mice after *S. pneumoniae* infection

In order to detect potential differences in tissue architecture between the two genotypes, we isolated lungs 72h post intra-nasal *S. pneumoniae* infection, fixed them in PFA and embedded the organs in paraffin. Tissue sections were then stained with haematoxylin and eosin.

In TTP$^{fl/fl}$ mice we observed considerably more and larger infiltrates of cells into the tissue (Fig. 5 A, B) compared to TTP$^{\Delta M}$ mice (Fig. 5 C, D). While there was quite a large variability between samples, the difference between genotypes was sufficiently pronounced to be visible by eye and to suggest that lack of TTP in the myeloid cell line reduced the local inflammation in the lung after *S. pneumoniae* infection. Immunohistochemical scoring could further be used to quantify the differences.

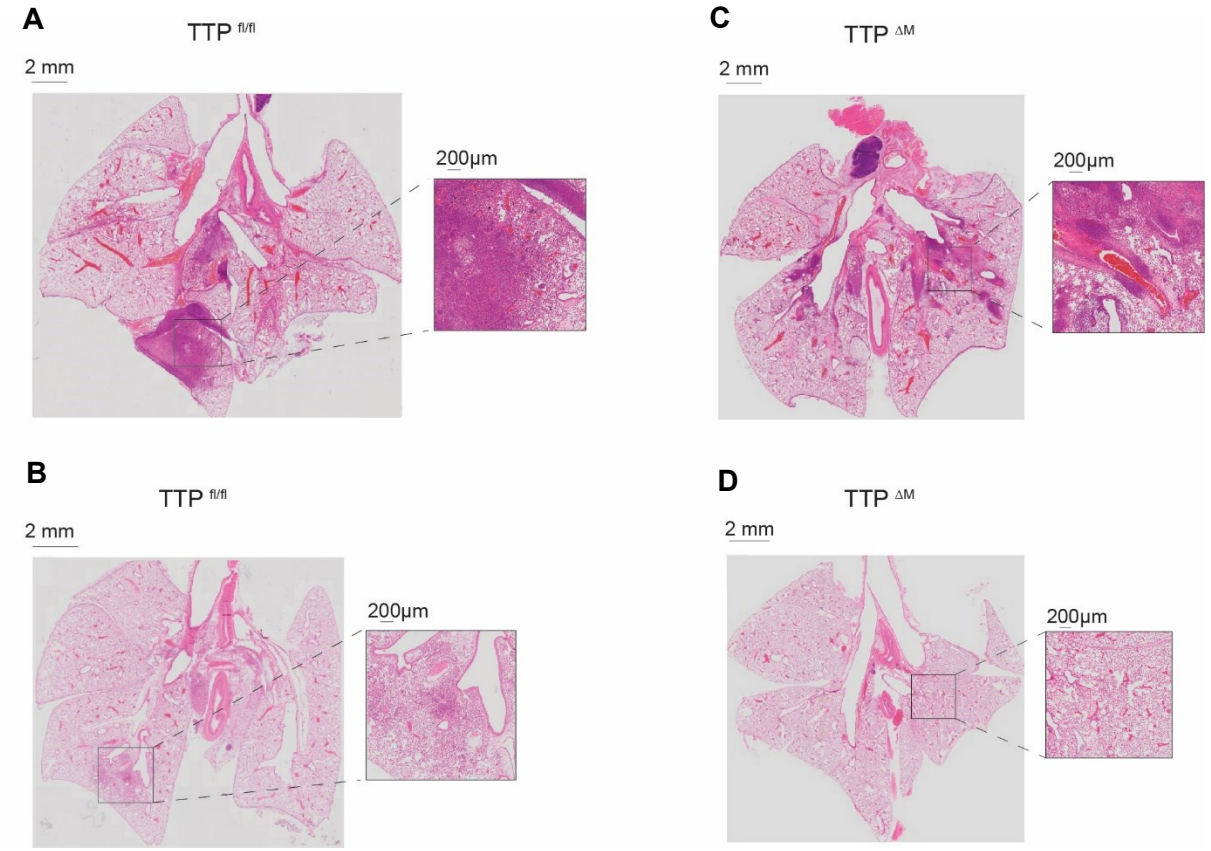

Fig. 5 Myeloid TTP increases cell infiltrates in tissue Mice were intra-nasally infected with *S. pneumoniae* and sacrificed 72h post-infection. Lungs were embedded in paraffin and tissue sections stained with haematoxylin and eosin. **A** Severe case of infiltration in TTP$^{fl/fl}$ mouse. **B** Rarer case of less severe infiltration in TTP$^{fl/fl}$ mouse. **C** More severe case of infiltration in TTP$^{\Delta M}$ mouse. **D** Common case of no infiltration in TTP$^{\Delta M}$ mouse. Data generated by Martina Borroni and Nora Bischoff.

Additionally, $TTP^{fl/fl}$ lungs contained higher levels of live bacteria 72h after infection (Fig. 6A). A lack of myeloid TTP apparently directly promoted pathogen reduction in the lungs as well as in more distant organs such as blood, kidney, liver (data not shown) and spleen (Fig. 6B).

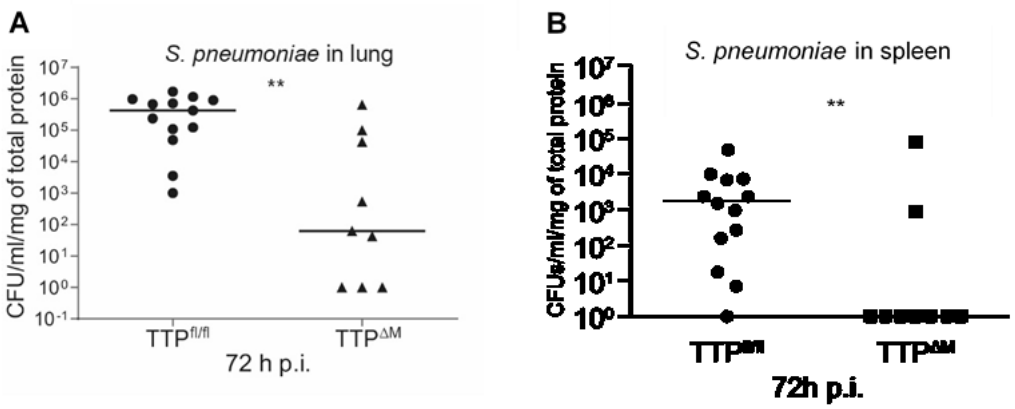

Fig. 1 Myeloid TTP reduces bacterial growth and spread $TTP^{fl/fl}$ and $TTP^{\Delta M}$ mice were infected intra-nasally with *S. pneumoniae* and sacrificed 72h post-infection. **A** CFUs of *S. pneumoniae* in the lung, n ($TTP^{fl/fl}$) = 13, n ($TTP^{\Delta M}$) = 9. **B** CFUs of *S. pneumoniae* in spleen, n ($TTP^{fl/fl}$) = 13, n ($TTP^{\Delta M}$) = 9. Data generated by Maša Ivin.

4.1.3 **Higher cytokine levels in $TTP^{\Delta M}$ mice**

Although we see reduced cell infiltration and better clearance in $TTP^{\Delta M}$ mice, the levels of cytokines such as IL-1β is higher. We detected higher levels of IL-1β mRNA already in the lung tissue of untreated mice (Fig. 7A) and also the protein amounts seem to be higher (Fig. 7D), but these results have to be validated with a more sensitive method, because the cytokine concentration in some samples was too low to be quantified with ELISA. At later time points of infection, no strong difference in IL-1β expression was observed as $TTP^{\Delta M}$ mice show only a slight increase in both mRNA and protein levels then (Fig. 7B, C, E, F). This finding is consistent with TTP's function of destabilizing cytokine mRNA such as *Il1b*[112]. However, it makes it even harder to reconcile this observation with the reduction in cell infiltration (and consequent tissue damage) observed in $TTP^{\Delta M}$ mice.

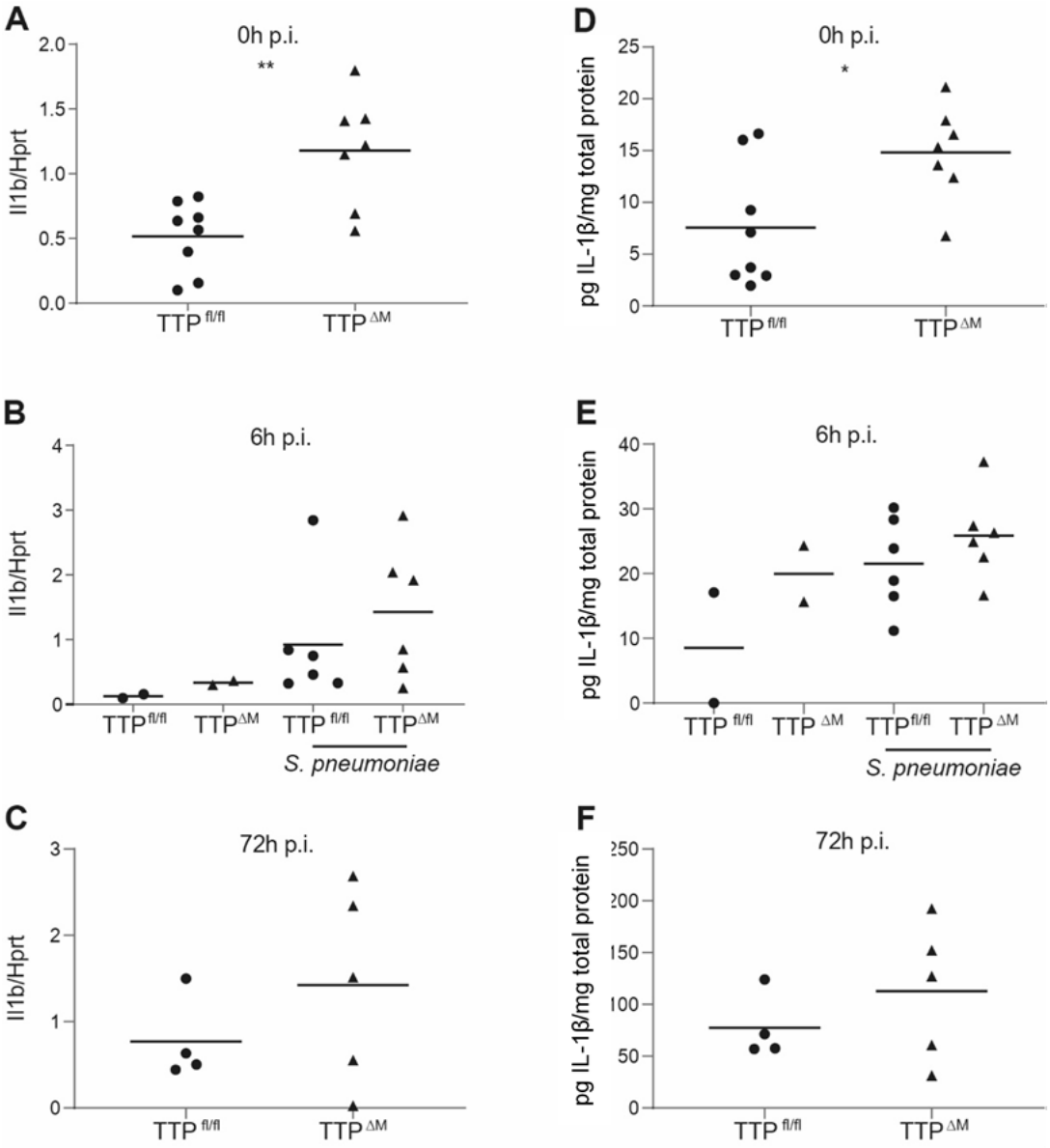

Fig. 7 Differential expression of IL-1β in TTP$^{fl/fl}$ and TTP$^{\Delta M}$ mice A-C IL-1β mRNA expression 0h, 6h and 72h post *S. pneumoniae* infection. **D-F** IL-1β protein expression 0h, 6h and 72h post *S. pneumoniae* infection. Data generated by Martina Borroni and Nora Bischoff.

4.1.4 Higher expression of Amphiregulin and phagocytosis promoting genes in TTP$^{\Delta M}$ mice

Based on the phenotype observed in TTP$^{\Delta M}$ mice, we hypothesize that TTP might restrain the bactericidal activity of myeloid cells on one side and on the other side negatively affect tissue protective functions. Support for this idea comes from RNA-seq studies and subsequent gene set enrichment analyses (GSEA). When the transcriptome of LPS stimulated alveolar macrophages isolated from TTP$^{fl/fl}$ and TTP$^{\Delta M}$ was compared, several genes were more expressed in the knock-out cells, a list of which can be found in figure 8E. Among these upregulated genes we could find *Areg* which codes for amphiregulin, a growth factor that binds to the EGF receptor, and some genes involved in positive

regulation of phagocytosis (Fig. 8D), such as *MARCO*, coding for a scavenger receptor (Fig. 8C). While in the RNA-sequencing study we saw higher *Areg* levels in TTP-deficient alveolar macrophages only prior to LPS stimulation (Fig. 8A), measuring mRNA levels using qPCR we also observed a difference after 3h LPS stimulation (Fig. 8B).

Amphiregulin is a tolerance promoting factor associated with tissue repair and resolution of inflammation, while phagocytosis is a mechanism of resistance against pathogens. We pursued both possible mechanisms (tolerance and resistance) to determine their contribution to the increase in survival rates seen in $TTP^{\Delta M}$ mice.

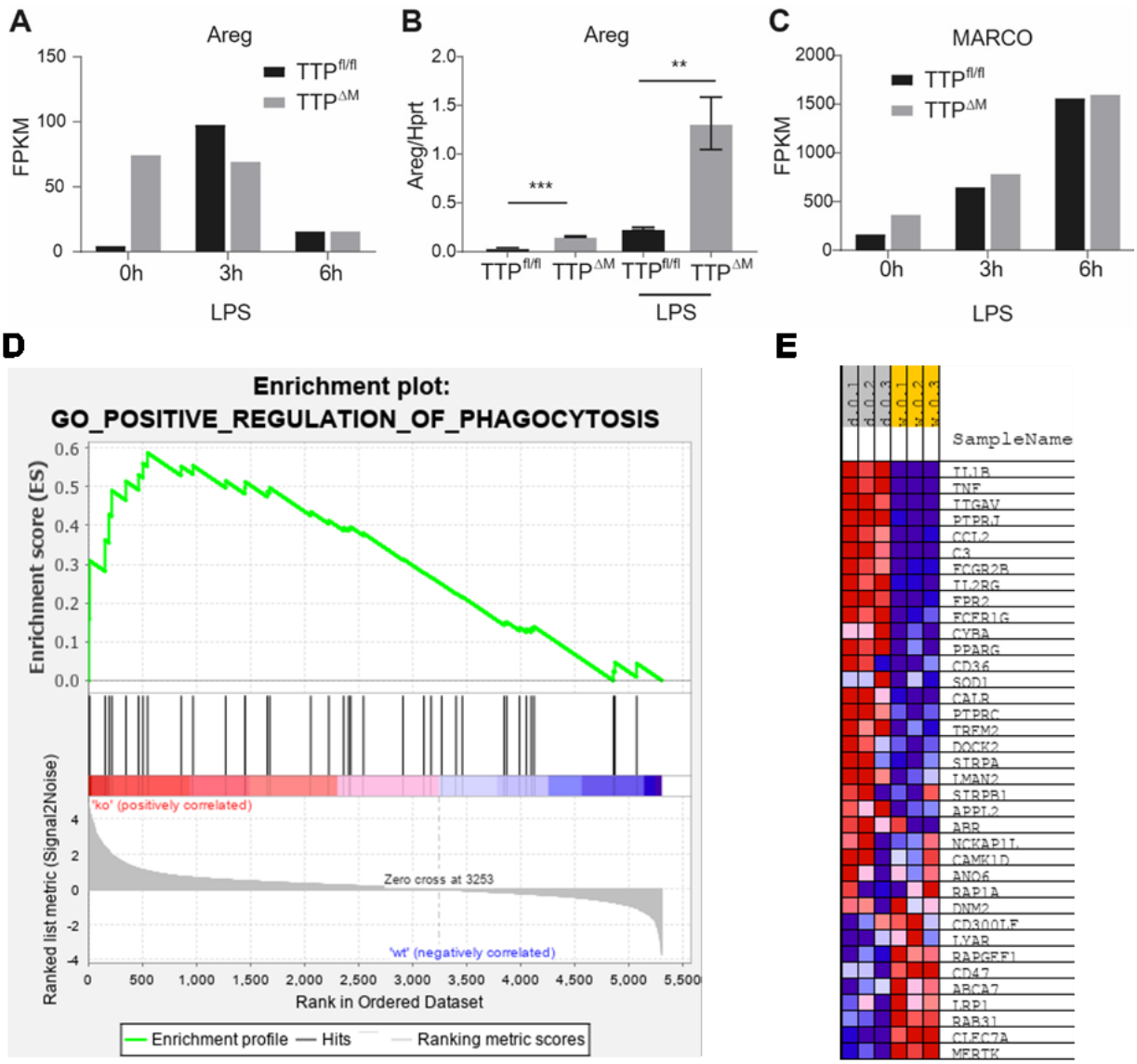

Fig. 8 Differential expression of amphiregulin and phagocytosis related genes A *Areg* expression in alveolar macrophages from RNA sequencing. **B** Areg mRNA expression in alveolar macrophages before and after 3h LPS stimulation. **C** MARCO mRNA expression in alveolar macrophages from RNA-sequencing. **D** GSEA of positive regulation of phagocytosis in alveolar macrophages without LPS stimulation. ES (Enrichment score): 0,58776104, NES (Normalized ES): 1,6143675 **E** List of genes differentially expressed in alveolar macrophages without LPS stimulation. (d...$TTP^{\Delta M}$, w...$TTP^{fl/fl}$), n = 3. Data generated by Martina Borroni.

4.2 Amphiregulin as TTP-regulated tolerance factor

4.2.1 Areg mRNA stability assays with TTP were inconclusive

Amphiregulin is upregulated in TTP knock-out alveolar macrophages both before and after LPS stimulation. To determine whether *Areg* is a direct TTP target and therefore destabilized by it, we decided to clone a reporter vector including the 3'UTR of *Areg* downstream of a luciferase gene whose expression could be controlled by doxycycline (Detailed description of cloning and plasmid map can be found in *6 Methods*).

HEK 293T cells were transfected with plasmids containing *Zfp36* coding for TTP, *rtTA* (the transactivation molecule for the tetracycline-responsive element in the *Areg* reporter vector) and the reporter construct itself. Reporter vectors containing the 3'UTR of *Il1a* or *Hprt* behind a luciferase gene were used as positive and negative control respectively because *Il1a* is a known TTP target and *Hprt* is not. After overnight treatment with doxycycline to induce reporter construct expression, transcription was stopped with actinomycin D and the RNA was isolated 0, 45 and 90 min later.

In such assays the ratio of TTP to target mRNA is important for optimal TTP mRNA destabilizing activity, therefore two different ratios of TTP plasmid to reporter plasmid were evaluated. TTP : reporter = 1 : 4 (Fig. 9A) and 1 : 15 (Fig. 9B), whereby the former seemed to produce slightly better results, although luciferase mRNA levels decreased by similar amounts independent from the 3'UTR it was fused to.

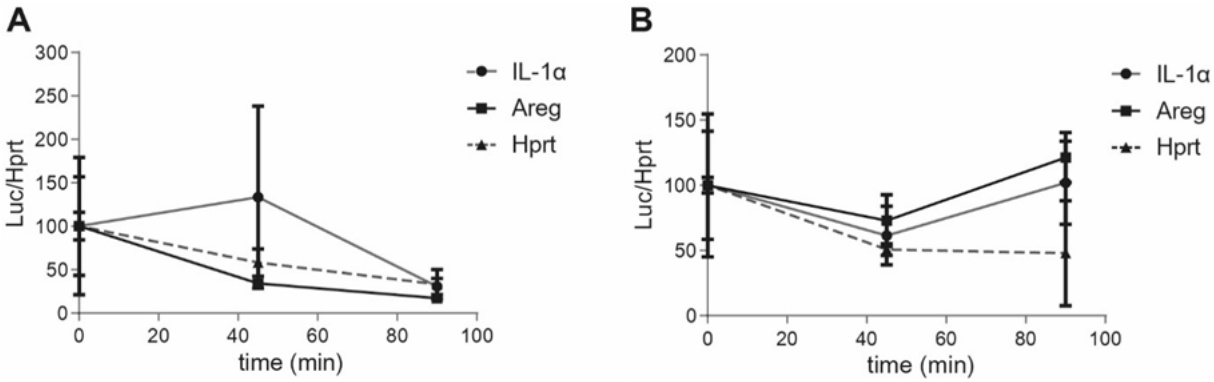

Fig. 9 Decay of luciferase mRNA fused to *Il1a*, *Hprt* or *Areg* 3'UTR in HEK 293T cells after transcription stop. **A** Cells transfected in a TTP : target ratio of 1:4. **B** Cells transfected in a TTP : target ratio of 1:15.

We expected the reporter fused to *Il1a* 3'UTR to degrade faster in cells with TTP compared to cells without TTP, whereas we didn't expect any change in stability for the reporter containing *Hprt* 3'UTR.

Unfortunately, the mRNA stability assays yielded inconclusive results, in part even showing higher levels of mRNA in samples from later timepoints. The decay rate of luciferase mRNA linked to the *Hprt* 3'UTR was comparable to the expected results for the positive control, so we couldn't draw any conclusion on the effect of TTP on *Areg* stability (Fig. 10B).

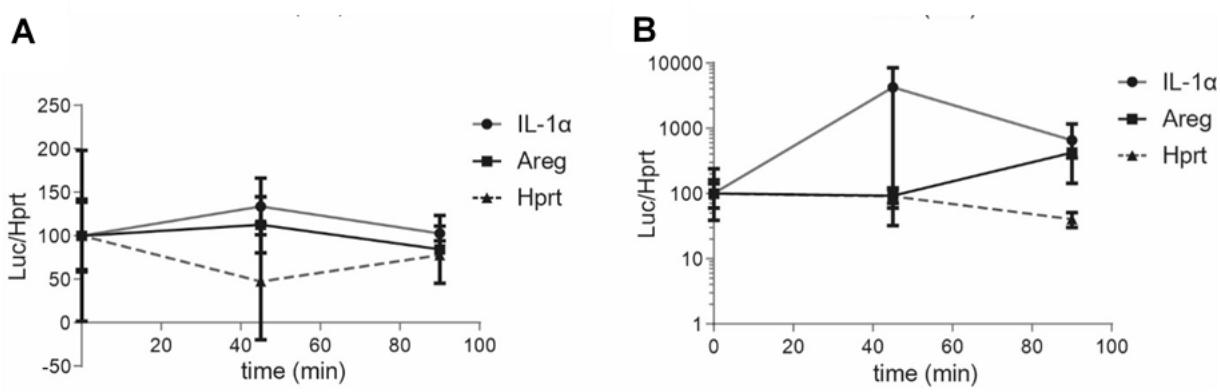

Fig. 10 A Cells tansfected in a 1:4 ratio of empty vector (replacing TTP) to target (3'UTR of *Il1a, Hprt* or *Areg*). **B** Cells transfected in a TTP : target ratio of 1:4.

One of the reasons for the high variability observed might be the low chance of all three plasmids entering enough cells. Transfection efficiency of HEK 293T cells was tested using flow cytometry, showing that 36.1% of cells were transfected when 1µg of DNA was used, which increased to 51.2 and 58.3% when 2 and 3µg DNA were used (Table 2). This means that the probability of a cell to be successfully transfected with three different plasmids lies between 4.6% (for 1µg DNA) and 19.5% (for 3µg DNA). Transfecting with too much DNA, however, often poses a problem when isolating RNA and an extra effort has to be made to remove all leftover DNA from the plasmids. In order to reduce the number of plasmids required, we tested transfection efficiency in Flp-In 293 *T-REx* (T-REx) *cells, which express TTP in a doxycycline inducible manner and would only require transfection with the reporter plasmid.* Transfection efficiency in these cells ranged from 8.8 to 29.1% which was still insufficient (Table 2).

Table 2 Transfection efficiencies depending on amount of DNA

Cell type	Plasmid DNA (Cop-GFP) (µg)	Transfected cells (%)
HEK 293T	1	36.1
HEK 293T	2	51.2
HEK 293T	2.5	53.8
HEK 293T	3	58.3
T-REx	1	12
T-REx	2	25
T-REx	2.5	26.6
T-REx	3	29.1
T-REx TTP	1	8.8
T-REx TTP	2	18.7
T-REx TTP	2.5	19.4
T-REx TTP	3	20.6

Different transfection methods did not improve the transfection efficiency in HEK 293 or T-REx cells (Table 3): standard transfection procedure of attached cells using polyethylenimine (PEI) or Fugene was most effective, compared to a transfection method which includes adding the transfection mix to the cells in suspension and then seeding them.

Table 3 Transfection efficiencies depending on transfection method (using 2µg Cop-GFP plasmid)

Cell type	Transfection method	Transfected cells (%)
HEK	PEI	56.3
HEK	PEI, suspension	55.4
HEK	Fugene	51
HEK	Fugene, supension	52.9
T-REx TTP	PEI	22.6
T-REx TTP	PEI, suspension	11.1
T-REx TTP	Fugene	29
T-REx TTP	Fugene, suspension	16,5

4.2.2 PAR-CLIP studies aiming to show *Areg*-TTP binding were inconclusive

A more direct proof for TTP binding to Areg mRNA can be attained by immunoprecipitation studies. Therefore, we wanted to test *Areg* presence in the pull-down with anti-TTP antibodies using photoactivatable ribonucleoside enhanced–cross linking and immunoprecipitation (PAR-CLIP). We first tested the method in HEK 293T cells, transfecting them with TTP, tetracycline transactivator and reporters containing a luciferase gene and either 3'UTRs of *Il1a* or *Hprt*. Looking at figure 10A one might think that the method works in principle as more luciferase mRNA was pulled down when it contained *Il1a* 3'UTR. However, similar ct values in input and no reverse transcriptase (RT) control meant that the results were not totally reliable (Fig. 10B).

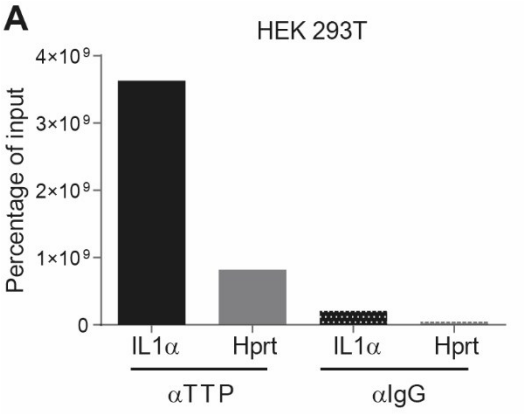

B

Sample	Ct value
Il1a αTTP	21.15
Il1a αIgG	24.51
Hprt αTTP	22.31
Hprt aIgG	25.76
Input *Il1a*	32.48
Input *Hprt*	32.16
No RT IP	32.21
No RT Input	27.35

Fig. 11 PAR-CLIP in HEK 293T cells according to protocol in *Methods* with a second DNase treatment **A** Luciferase mRNA in pull-down normalized over input. **B** Ct values of luciferase mRNA.

This was confirmed when different conditions were tested, which in theory would not lead to increased pull-down of luciferase mRNA: We only transfected with *Il1a* reporter plasmid (unstimulated or stimulated with doxycycline), with reporter and TTP plasmid (but without doxycycline treatment) and with TTP only. As expected, there was no increased pull-down of luciferase mRNA compared to IgG controls (Fig. 12A). While there was also no signal in the no RT control this time, the cycle numbers of the input samples where we would expect a signal (samples transfected with *Il1a* stimulated with doxycycline) were too high and there was no difference between these samples and other input samples (especially unstimulated samples transfected with *Il1a*) (Fig. 12B).

A

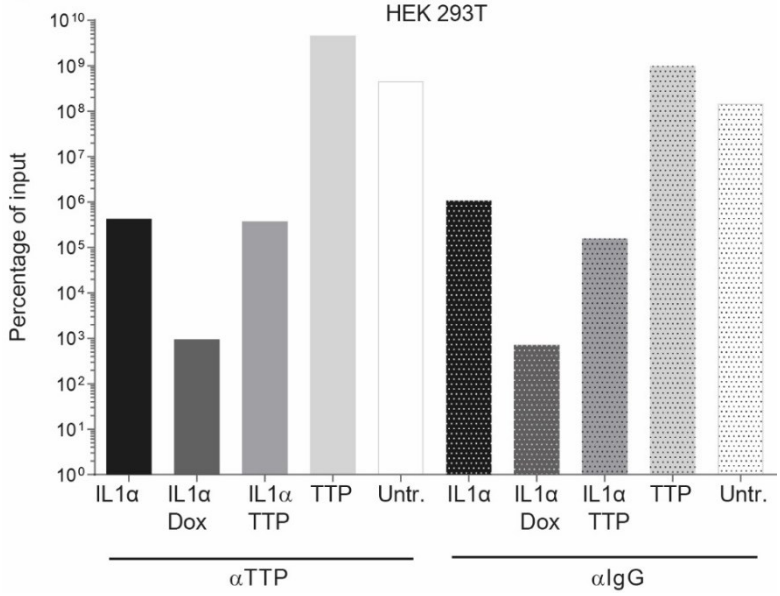

B

Sample	Ct value
Input *Il1a*	30.62
Input *Il1a* Dox	29.7
Input *Il1a* TTP	29.09
Input TTP	38.86
Input untransfect.	39.22
No RT	N/A

Fig. 12 PAR-CLIP in HEK 293T cells according to protocol in *Methods*. **A** Luciferase mRNA in pull-down normalized over input. **B** Ct values of luciferase mRNA in input samples.

Similar issues with too high cycle numbers were encountered in experiments with RAW macrophages. We focused only on the input to see if we could decrease ct values by different methods. TTP induction worked, as can be seen in the western blot in figure 13, where TTP is only expressed in WT cells upon LPS stimulation.

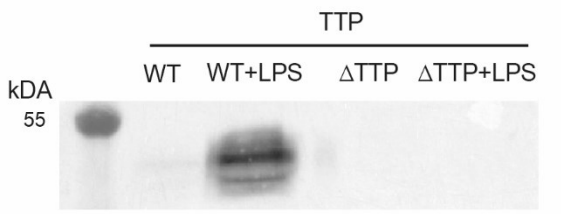

Fig. 13 TTP expression in RAW macrophages (WT and ΔTTP) unstimulated or stimulated with LPS for 3h.

Furthermore, LPS stimulation can be seen in figure 14A, as there is only signal in LPS stimulated samples. Therefore, LPS treatment could be excluded as possible error source.

Even in the input (without additional procedural steps for the pull-down that could cause RNA loss) cycle numbers for *TNF* were too high. Only directly isolating RNA using acidic phenol/chloroform generated lower ct values for both *TNF* and *Hprt*, but this interestingly resulted in lowest *TNF* levels after normalization. Adding a proteinase K digestion step already prevented the generation of lower ct values. Using an enhanced reverse transcriptase to produce cDNA (SuperScript IV reverse transcriptase from ThermoFisher) didn't improve the yield and *Il1a* could not be detected at all (Fig. 14B).

A

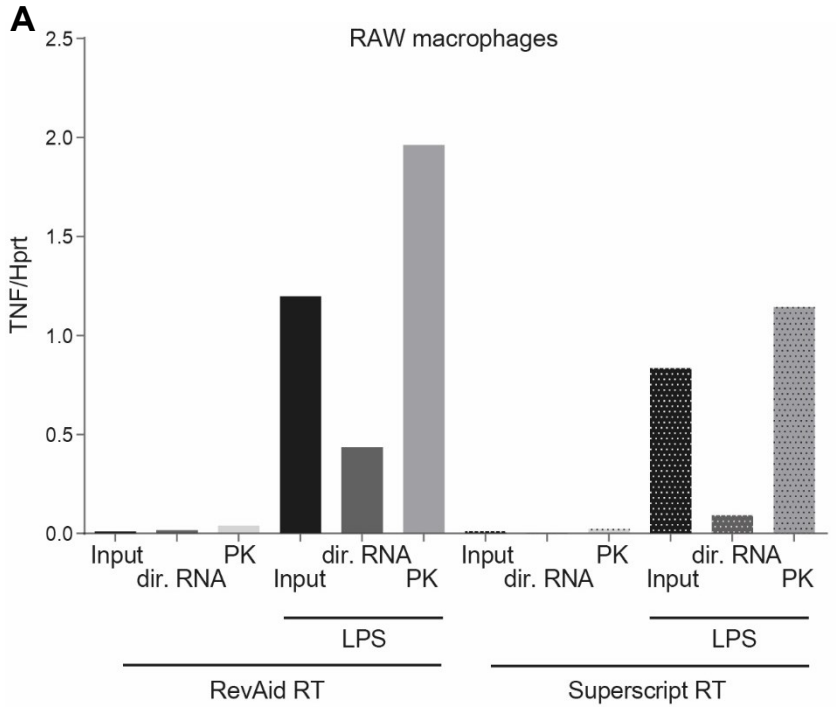

B

Sample	*TNF*	*Hprt*	*Il1a*
Input LPS	27.34	30.37	N/A
Input	34.34	31.82	N/A
Dir. RNA LPS	23.20	23.22	N/A
Dir. RNA	27.29	23.42	N/A
Dir. RNA PK LPS	27.24	31.03	N/A
Dir. RNA PK	32.51	31.51	N/A
No RT Input	35.11	37.22	N/A
No RT dir. RNA	37.14		

Fig. 14 RAW macrophages treated with LPS, samples treated as PAR-CLIP input according to standard protocol (Input), by directly isolating RNA (adding acidic phenol-chloroform directly after lysis) (dir. RNA) and by directly isolating RNA after proteinase K (PK) digestion (adding PK after lysis and then adding acidic phenol-chloroform) (dir.RNA PK). RNA transcribed to cDNA using either RevAid RT or SuperscriptRT. **A** *TNF* levels. **B** Ct values of *TNF*, *Hprt* and *Il1a* using RevAid RT.

Omitting DNase treatment or using a different lysis buffer did not have the desired effect (Fig. 15A, B). Furthermore, cross-linking did not seem to be responsible for RNA loss as skipping treatment with UV

light didn't shift the qPCR curves to the left (Fig. 15C). Moreover, this was not only the case for *TNF* but also for *Cxcl2* and *Il1a* for example which could not be detected at all.

A

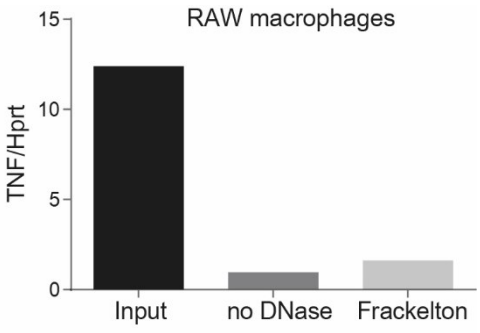

B

Sample	*TNF*	*Hprt*	*Cxcl2*	*Il1a*
Input LPS	27.34	30.37		N/A
Input	34.34	31.82		N/A
Dir. RNA LPS	23.20	23.22		N/A
Dir. RNA	27.29	23.42		N/A
Dir. RNA PK LPS	27.24	31.03		N/A
Dir. RNA PK	32.51	31.51		N/A
No RT Input	35.11	37.22		N/A
No RT dir. RNA	37.14			

C

RIP Input	32.59	34.61	31.70	N/A
RIP No RT	N/A	N/A	N/A	N/A

Fig. 15 RAW macrophages treated with LPS, samples treated as PAR-CLIP input according to standard protocol, according to standard protocol omitting DNase treatment or using Frackelton lysis buffer while also omitting DNase treatment. **A** *TNF* levels. **B** Ct values of *TNF*, *Hprt* and *Il1a*. **C** RAW macrophages treated with LPS and samples treating according to PAR-CLIP input protocol without cross-linking. Ct values of *TNF*, *Hprt*, *Cxcl2* and *Il1a*.

Therefore, we tried to find endogenous targets of TTP in HEK 293T cells, which could help us establish the method despite the limited biological relevance of such targets. *ADAMTS1* and *JUN* were chosen due to their differential expression in HEK 293T cells in absence and presence of TTP according to Mukherjee et al. (2014)[173]. Both could be detected in RNA isolated directly from HEK 293T cells with cycle numbers between 24 and 26. When RNA was gained using the RIP procedure however, only *JUN* could be detected in very low amounts (ct = 36.34, no RT: ct = 38.31), again showing that during the processing with PAR-CLIP buffers RNA is lost or degraded.

4.3 TTP regulating resistance mechanisms

4.3.1 No increase in macrophage or neutrophil number in broncho-alveolar lavage in $TTP^{\Delta M}$ as compared to $TTP^{fl/fl}$

Moving on from tolerance to resistance mechanisms that could be limited by myeloid TTP, we entertained the possibility of higher immune cell numbers at the infection site that can eliminate the pathogens. Therefore, the number of immune cells in the broncho-alveolar lavage (BAL) of mice was examined using flow cytometry. We observed no difference in neutrophil or alveolar macrophage abundance between $TTP^{\Delta M}$ and wild type mice, neither prior (Fig. 16 A, C), nor 24h post *S. pneumoniae* infection (Fig. 16 B, D). Previous experiments by Martina Borroni analysing whole lung tissue also showed no differences between the genotypes (data not shown). These results contrast with our finding of increased infiltration in wild type mice; following this we would expect to find more immune

cells at the infection site. Flow cytometry data point towards a different reason for more effective bacterial elimination than simply more phagocytic cells in TTP$^{\Delta M}$ mice. Rather, it suggests that the function of these cells is enhanced and that they can therefore kill bacteria more effectively.

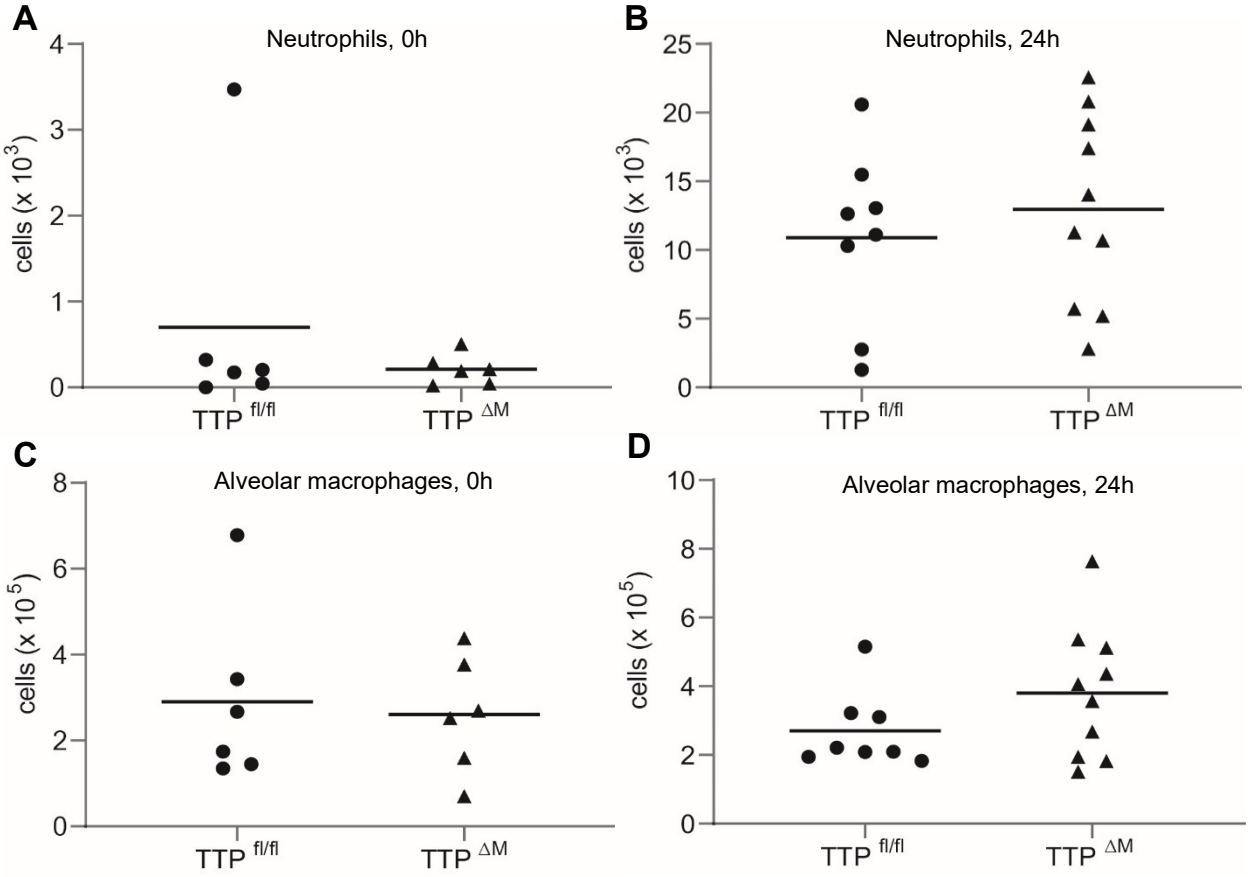

Fig. 16 No increase in immune cell number in BAL A Neutrophils at timepoint 0h (no *S. pneumoniae* infection). **B** Neutrophils 24h post *S. pneumoniae* infection (10^4 CFUs/mouse). **C** Alveolar macrophages at 0h. **D** Alveolar macrophages 24h post-infection. **A-D** Data generated by Nora Bischoff and Martina Borroni.

4.3.2 **Myeloid TTP decreases phagocytic activity of macrophages in vitro**

This let us pursue the idea that increased phagocytosis by macrophages leads to increased survival rates in TTP$^{\Delta M}$ mice. For phagocytosis assays various types of macrophages were incubated with dyed heat-killed bacteria and then analysed by flow cytometry. As a negative control, cells were incubated at 4°C and not-internalized bacteria were removed by extensive washing.

TTP-deficient RAW macrophages as well as BMDMs and alveolar macrophages from TTP$^{\Delta M}$ mice exhibited increased phagocytosis of *S. pneumoniae* (Fig. 17).

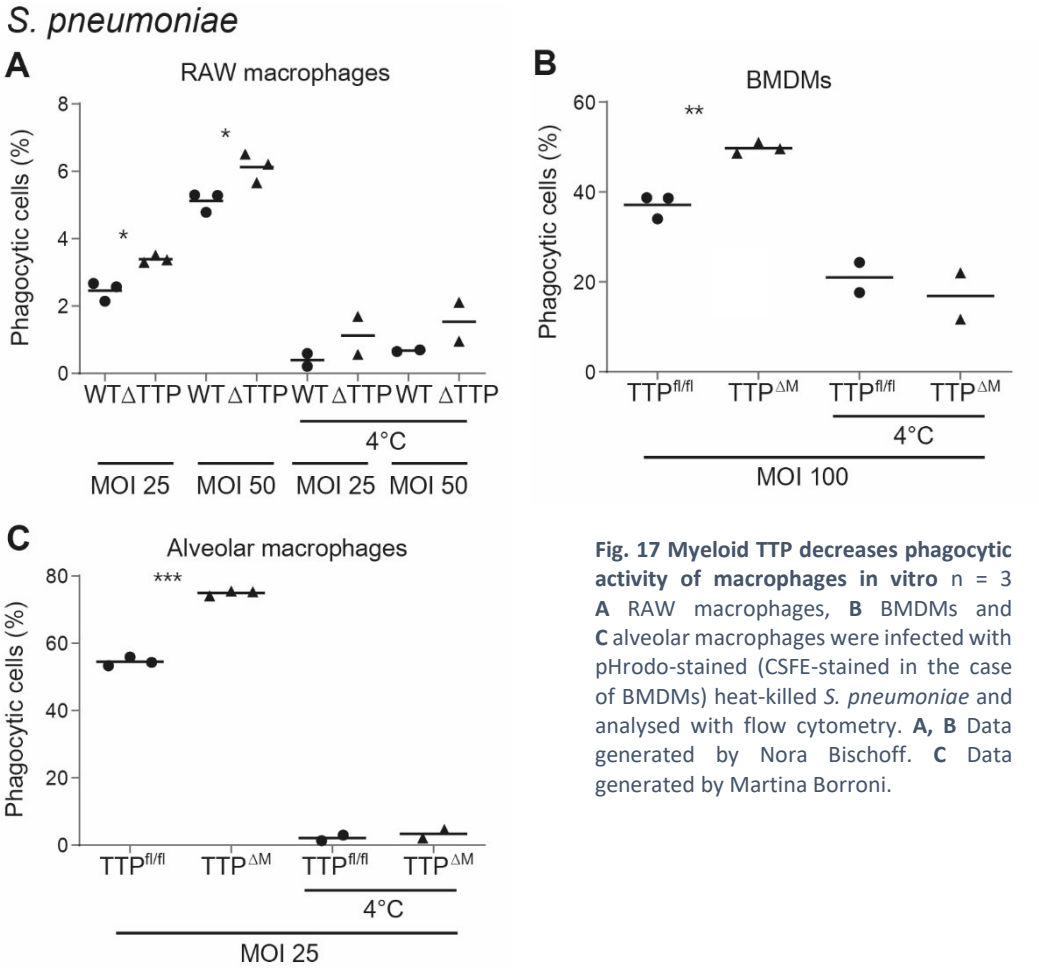

Fig. 17 Myeloid TTP decreases phagocytic activity of macrophages in vitro n = 3 **A** RAW macrophages, **B** BMDMs and **C** alveolar macrophages were infected with pHrodo-stained (CSFE-stained in the case of BMDMs) heat-killed *S. pneumoniae* and analysed with flow cytometry. **A, B** Data generated by Nora Bischoff. **C** Data generated by Martina Borroni.

The response was also tested with *S. pyogenes* in RAW macrophages and BMDMs, with similar results although the difference between genotypes seems to be a bit smaller in BMDMs, though still significant (Fig. 18).

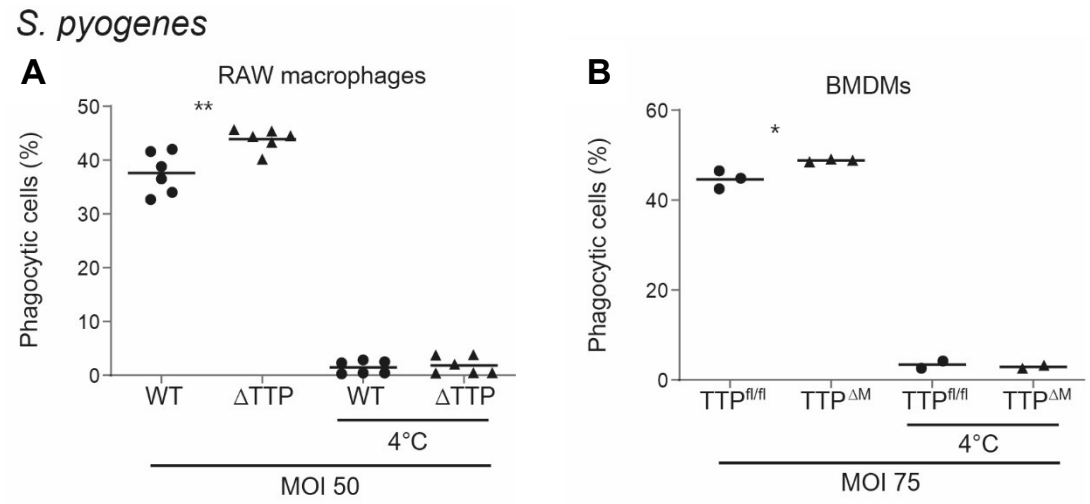

Fig. 18 Myeloid TTP decreases phagocytic activity of macrophages in vitro A RAW macrophages (n = 6 from two independent experiments) and **B** BMDMs were infected with CFSE-stained heat-killed *S. pyogenes* and analysed with flow cytometry. **A** Data generated by Nora Bischoff. **B** Data generated by Martina Borroni.

The percentages of phagocytic cells all fall in a similar range of about 40 to 50%, just alveolar macrophages exhibit 60 to 70% phagocytic cells. At first we used pHrodo to dye the bacteria, which has the advantage that it gives off the strongest signal when in an acidic environment, thereby showing that bacteria are not only taken up by cells, but that the phagosome also progresses to the mature bacteria-digesting organelle. Unfortunately, it produced an unfavourable signal to noise ratio and no reproducible results in primary cells. This also explains the low number of phagocytic cells in RAW macrophages in Fig. 17A. Most data, except Fig. 17A (RAW macrophages) and Fig. 17C (alveolar macrophages), were acquired using CFSE-dyed bacteria, which showed a stronger and more consistent signal.

4.3.3 Increased phagocytosis in absence of TTP is independent of bacteria-recognizing receptors

To test whether the increase in phagocytosis is dependent on specific bacteria-recognizing receptors or pathogen-induced signalling, I performed phagocytosis assays using fluorescent latex beads. Incubating RAW macrophages with beads produced consistent and reproducible results, which show higher phagocytic activity in TTP knock-out cells compared to wild type (Fig. 19A). The increased phagocytosis observed in ΔTTP RAW macrophages reflects what has been observed in alveolar macrophages (Fig. 19B).

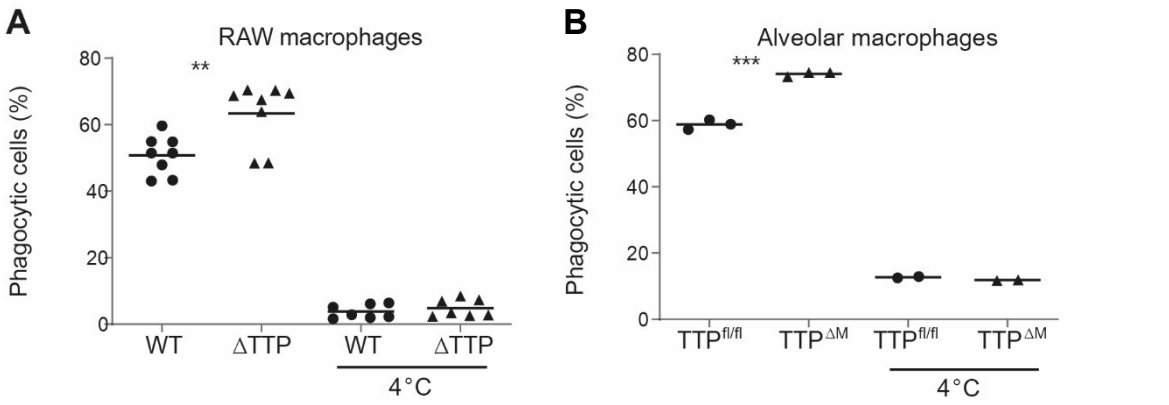

Fig. 19 Immuno-signalling independent phagocytosis Macrophages were incubated with fluorescent beads, MOI 50, and analysed with flow cytometry. **A** RAW macrophages, n = 8 from three independent experiments. Data generated by Nora Bischoff. **B** Alveolar macrophages, n=3. Data generated by Martina Borroni.

I also assessed phagocytosis using a second method, namely measuring fluorescent intensity of internalized beads using a plate reader. While the results are not as clear as those generated from flow cytometry, the data show the same trend of higher phagocytic activity in ΔTTP cells (Fig. 20).

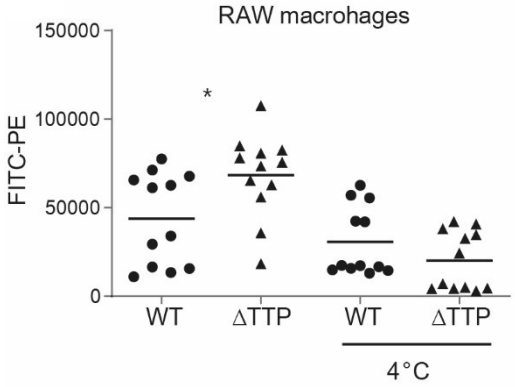

Fig. 20 RAW macrophages were incubated with fluorescent beads, MOI 50, and analysed with a plate reader. n = 6 from two independent experiments. Data generated by Nora Bischoff.

So far, no difference in phagocytic uptake of beads was detected between $TTP^{fl/fl}$ and $TTP^{\Delta M}$ BMDMs using flow cytometry (Fig. 21A). I also measured bead fluorescence with the plate reader, as we suspected that BMDMs might need to be seeded on tissue-culture treated dishes to exploit their full phagocytic potential. Still, this approach yielded the same results, namely that that there is no observable difference in phagocytic behaviour between the genotypes of BMDMs (Fig. 21B).

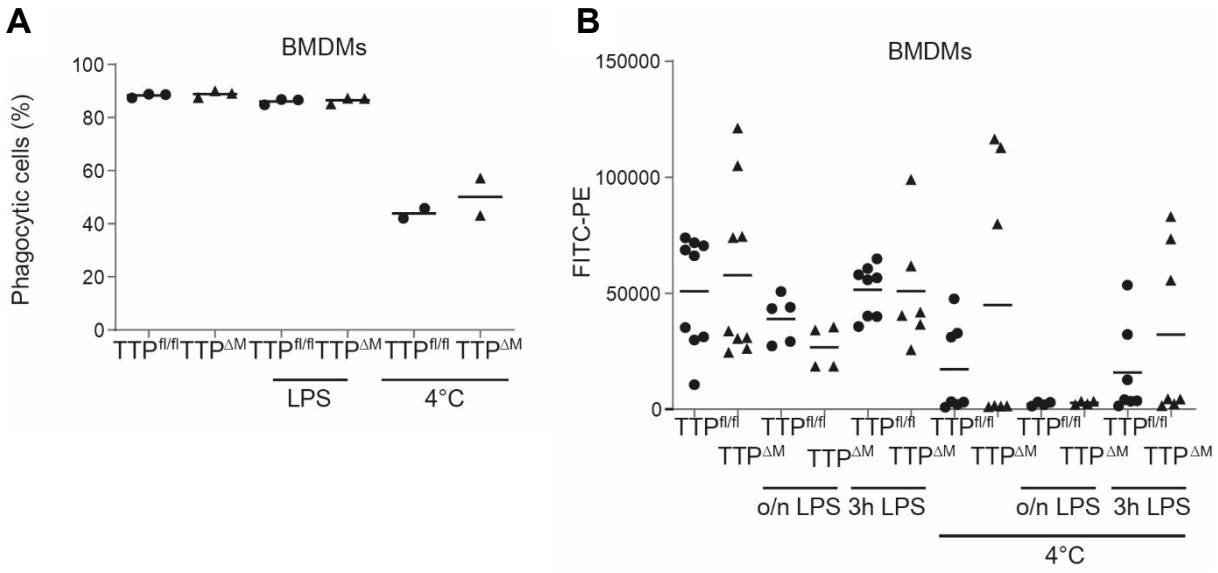

Fig. 21 BMDMs were incubated with fluorescent beads, MOI 50. **A** Flow cytometry, 3h LPS treatment, n = 6 from two independent experiments. **B** Plate reader, n = 4-9 from two independent experiments (one in the case of overnight LPS). Data generated by Nora Bischoff.

To conclude, RAW macrophages and alveolar macrophages likely do not depend on specific bacteria-recognizing receptors for increased phagocytosis in absence of TTP while the same cannot be said for BMDMs.

4.3.4 LPS stimulation has no effect on phagocytic activity in RAW macrophages or BMDMs

We suspected that immunologically primed macrophages might be better able to take up particles, because some signalling pathways have already been activated and they are already in a more active state. It has been reported that previous macrophage stimulation lead to persistent enhancers on the chromatin and cells responded to renewed stimulus with faster and stronger activation[174]. Also, *Drosophila* infected with sublethal doses of *S. pneumoniae* survived higher doses of the pathogen throughout their lives, and phagocytes are involved in this pathogen-specific immunity[175]. However, there is also evidence that LPS pre-treatment does not change gene expression after follow-up LPS stimulation[176].

To test the effects of LPS stimulation on our model, macrophages were stimulated with LPS for 3h or overnight before adding the beads. However, this didn't seem to have any effect on phagocytic activity. In RAW macrophages, presence of TTP still decreased phagocytosis but by the same amount as it did without LPS priming (Fig. 22). In BMDMs I still didn't detect any difference in phagocytic activity between wild type and TTP-deficient cells, neither using flow cytometry (Fig. 21A) or the plate reader (Fig. 21B) for analysis.

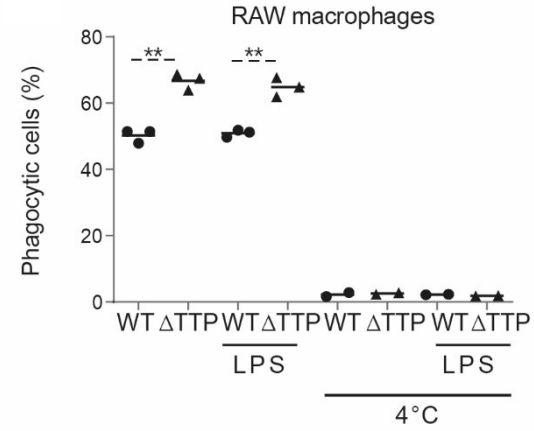

Fig. 22 RAW macrophages were stimulated with LPS for 3h, incubated with fluorescent beads, MOI 50, and analysed with flow cytometry, n = 3.

4.3.5 No increased killing of internal bacteria in TTP-deficient macrophages

As phagocytosis in TTP-deficient macrophages is increased, we hypothesized that also the killing of phagocytized bacteria could be affected and that this could additionally contribute to increased survival rates of $TTP^{\Delta M}$ mice challenged with *S. pneumoniae* lung infection.

To test macrophage capacity to kill internal bacteria, BMDMs of $TTP^{fl/fl}$ and $TTP^{\Delta M}$ mice were incubated with live *S. pneumoniae* (MOI 25) for an hour, after which external bacteria were removed and cells were lysed immediately or 15min and 30min later. Intracellular bacteria, that were thereby released,

were plated and CFUs counted. There was a large variation among samples and the results are not entirely conclusive, one time showing fewer surviving bacteria in $TTP^{\Delta M}$ cells (Fig. 9A) while another timer showing no difference between genotypes (Fig. 9B). According to the current status it seems more likely that TTP has no significant effect on the ability of macrophages to kill the bacteria they ingested although more experiments are needed to confirm this supposition.

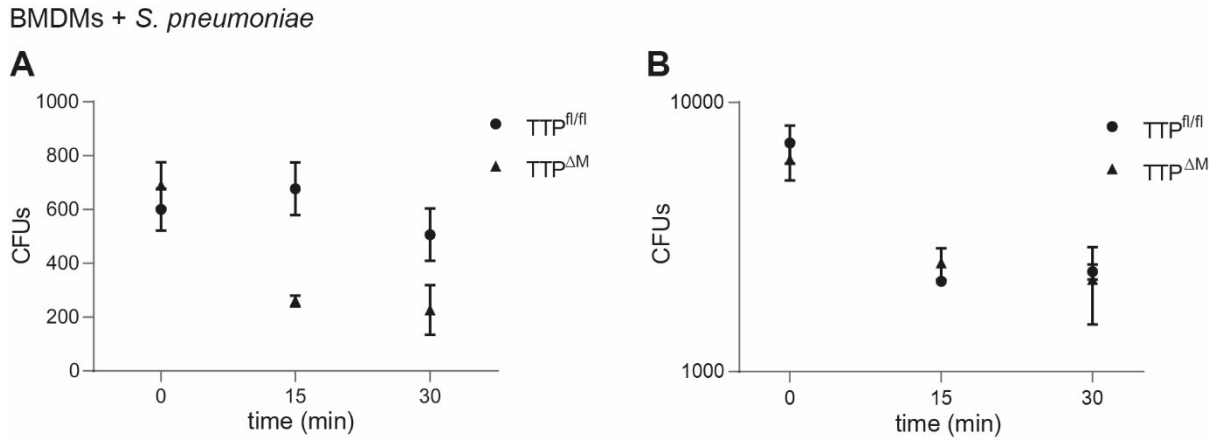

Fig. 23 Killing of internal bacteria BMDMs were infected with live *S. pneumoniae* (MOI 25), external bacteria were killed and cells were lysed at different time points afterwards to release internal bacteria. CFUs were calculated using the Miles and Misra method. **A** and **B** are biological replicates, (n = 3). Data generated by Martina Borroni and Nora Bischoff.

5 Conclusion and Discussion

5.1 Amphiregulin as a TTP target

Amphiregulin has not been identified as a TTP target in the TTP atlas by the stringent peak-finding algorithm used[76], but a distinct peak can be seen in the 3'UTR (Fig. 24). This, together with the finding that Amphiregulin is upregulated in TTP knock-out alveolar macrophages suggests that *Areg* might be targeted by TTP.

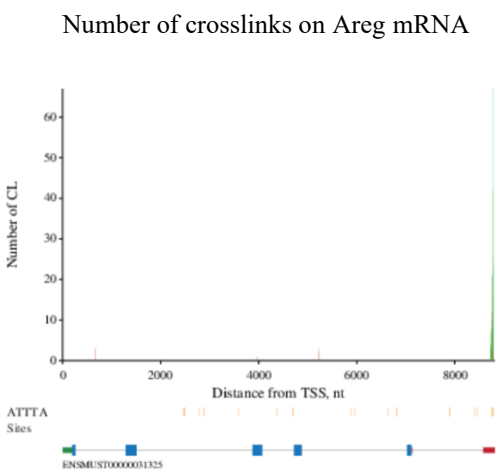

Fig. 24 PAR-iCLIP coverage for *Areg* from the TTP atlas[76]

Both mRNA stability and PAR-CLIP assays failed to show Amphiregulin as a TTP target. This is not to say that is isn't one, rather the methods need more extensive optimization. In the mRNA stability assays the transfection efficiencies seemed to be the biggest problem meaning that in too few cells all necessary plasmids were present in their desired ratio leading to confusing and unreliable results. Increasing the amount of plasmid DNA to 2µg was the most promising step, while different cell types and transfection methods did not bring improved results.

In the case of the PAR-CLIP, the problem lay in substantial RNA degradation. Although we measured high concentration of RNA in the samples prior to cDNA production, the ct values of the input samples were consistently too high during qPCR - probably owing to degradation. This could not be prevented by using a different lysis buffer, using more ribonuclease inhibitor or omitting the DNA digestion step; hence, the reaction buffers themselves seem to be the only possible cause.

Once the method is established, it could additionally be used to investigate whether phagocytosis related genes are direct TTP targets and if so whether this is cell type dependent. Candidates are for example *SLC4A7* (for which TTP binding sites have been found already) and *NOX2* (where results have not been clear)[76].

5.2 Myeloid TTP reduces phagocytic activity of macrophages in vitro

We didn't observe any difference in neutrophil and alveolar macrophage abundances in the broncho-alveolar lavage of $TTP^{fl/fl}$ and $TTP^{\Delta M}$ mice. The same observation was made when analysing the whole lung tissue. As we see more infiltrates in $TTP^{fl/fl}$ lungs, this poses the question whether the infiltrates are composed of different (immune) cells than neutrophils and alveolar macrophages. To specify the cell types present at the infiltrates, immunohistochemical stainings of the tissue slides should be performed. Immune cell numbers in the whole lung should also be quantified, to see whether there is

a difference there, even though relative abundances do not differ between genotypes. Despite some uncertainty regarding these findings, so far it seems that rather than cell number, cell activity (especially of macrophages) plays a role in the increased survival of lung infected $TTP^{\Delta M}$ mice.

An increase in phagocytosis could at least partially explain the phenotype observed in myeloid specific TTP knock-out mice in a lung infection model. Not only is the ingestion of pathogens the main function of macrophages but it could also serve as an explanation for three different observations: increased survival, reduced bacterial load in tissues and reduced tissue infiltration in $TTP^{\Delta M}$ mice in response to lung infection with *S. pneumoniae*. Although signalling during phagocytosis can lead to the expression of pro-inflammatory factors, phagocytosis itself doesn't contribute to tissue damage and is probably the safest and most effective way of dealing with a pathogen.

Here we show for the first time that TTP is involved in the regulation of phagocytosis and therefore that its function in regulation of the immune response is broader than previously thought. Macrophages lacking TTP consistently exhibit higher phagocytosis of heat-killed bacteria in vitro. This is true for RAW macrophages, BMDMs and alveolar macrophages incubated with both *S. pneumoniae* and *S. pyogenes*. As both of these are gram-positive pathogens, it would be interesting to test whether phagocytes respond similarly to gram-negative bacteria. For the most part, results of phagocytosis assays were very reliable, however, data from experiments with alveolar macrophages were not always reproducible. What could be a factor is that the cells for the phagocytosis assays were kept in culture overnight after the isolation and were therefore not part of the in vivo system for some time. It is possible that signalling pathways and phagocytosis related genes are influenced by this and further phagocytosis assay should be done with freshly isolated cells.

The hypothesis that TTP limits phagocytosis is in line with the finding that phagocytosis promoting genes are more expressed in TTP-deficient cells, even though phagocytosis is not a top hit in GSEA. Seeing as TTP is well known as an anti-inflammatory factor, it is conceivable that it decreases macrophage activity not only by decreasing their expression of cytokines but also by toning down their pathogen-ingesting ability.

An interesting gene found to be increased in TTP-lacking cells is *MARCO* (macrophage receptor with collagenous structure) which codes for a pattern recognition/scavenger receptor mainly recognizing polyanions and LDL and which could potentially play a role in increased phagocytosis. It is not expressed in RAW macrophages, however, that's why MARCO cannot come into play there. Also, there is no evidence of a TTP binding site in its mRNA.[76] The fact that beads are just as well taken up as heat-killed bacteria suggests that signalling induced by bacterial surface antigens and bacteria-recognizing factors is not responsible for the increase in phagocytosis observed in $TTP^{-/-}$ cells. Also, the finding that priming macrophages with LPS does not seem to have an effect indicates that the process by which

TTP hinders phagocytosis is independent from inflammatory stimulation. This corresponds to the expression profiles of alveolar macrophages in which the biggest difference in *MARCO* expression was observed prior to LPS stimulation. It could be interesting to stimulate cells with interferons instead of LPS to see whether this causes differences in phagocytosis.

Among the cell types analysed, BMDMs were an exception in that they didn't show different phagocytic activity between genotypes when incubated with beads, only when incubated with bacteria. If this is indeed the case and not just an effect of the experimental set-up which is quite removed from the situation in vivo, it might be an interesting finding. While both processes depend on FAK/Src and MAPK, phagocytosis of bacteria depends on RGD-binding receptors while latex bead uptake does not.[177] We know that there are differences between cell types regarding the effects of TTP, so it is plausible that TTP in BMDMs acts on phagocytosis in a different way which might be dependent on signalling caused by bacteria. *MARCO* expression for example is not increased in TTP-deficient BMDMs before or after LPS stimulation.[76]

5.3 No increased killing of internal bacteria by TTP-deficient macrophages

Although TTP-deficient macrophages take up bacteria better, we found no indication that they are also better (i.e. faster) at killing the ingested bacteria. The bicarbonate transporter SLC4A7 which is important for phagosome acidification in macrophages has been found to possess a TTP binding site in its mRNA[76], but this is rather an exception among proteins involved in phagosome maturation and it is entirely likely that TTP does not play a role in this process. It would make sense for both processes to improve as otherwise macrophages could get overwhelmed by the number of bacteria they take up. However, as the assays showed, most ingested bacteria had already been killed after 30min. This fast processing might be the reason why there is no need for more efficient bacterial killing in order to achieve the described effects in vivo.

Overall, this work shows TTP to be involved in the regulation of the immune response in more ways than just cytokine expression. The negative regulation of phagocytosis which is conserved over several macrophage types is in its detailed mechanisms likely to be cell type specific. Further testing with other macrophage types would give more weight to this argument and would maybe give us more insight into the differences between them. Why BMDMs but no other macrophages tested so far react differently to beads than to bacteria should be a subject of investigation.

6 Methods

6.1 Mice

Myeloid-specific TTP-deficient ($TTP^{\Delta M}$) mice were generated by crossing mice with *loxP*-flanked *Zfp36* ($TTP^{fl/fl}$) with mice expressing Cre recombinase under the control of the murine M lysozyme promoter, which is specific for cells of the myeloid lineage (LysMcre).[114] Neutrophil-specific TTP-deficient ($TTP^{\Delta N}$) mice were generated by crossing $TTP^{fl/fl}$ mice with mice expressing Cre under a neutrophil specific promotor. $TTP^{fl/fl}$ mice were used as wild type controls. All mouse lines had a B57BL/6 genetic background.

6.2 Cell lines and isolation of primary cells

RAW 264.7 and RAW 264.7 ΔTTP were cultured in Dulbecco's modified Eagle's medium with high glucose (DMEM, Sigma-Aldrich) with 10% fetal calf serum (FCS) and Penicillin/Streptomycin (50mg/ml / 100mg/ml) and split using a rubber scraper. HEK 293T and Flp-In™ T-REx™-293 cells (ThermoFisher) were kept in the same medium but split using a trypsin-EDTA solution (0.25% trypsin). Flp-In™ T-REx™-293 cells were selected with blasticidin (15µg/ml, InvivoGen) and zeocin (100µg/ml) and Flp-In™ T-REx™-293 cells in which TTP had been integrated were selected with blasticidin (15µg/ml) and hygromycin (100µg/ml) over approximately 6 days during which time they were not kept too densely on the plate as this would hinder the selection process.

Isolation of alveolar macrophages: Mice were sacrificed using CO_2 and their trachea exposed. A catheter was inserted and 10ml 0.9% NaCl solution were pumped into the lung in 0.5ml steps. The liquid was retrieved by a second syringe while massaging the lung lightly. Cells were spun down at 300rcf for 5min and cultured in RPMI with 10% FCS, Pen/Strep.

Isolation of BMDMs: Mice were sacrificed, and femur and tibia were isolated. The ends of the bones were cut off and the bones rinsed using syringes with pure DMEM to flush out the bone marrow. Cells were seeded in DMEM with 10% FCS, Pen/Strep and 30% L-conditioned medium, containing growth and differentiation factors.

6.3 Buffers

All PAR-CLIP buffers were prepared with nuclease-free water.

Par-Clip Lysis Buffer 5x: 250 mM Tris-HCl (pH 7.4), 500 mM NaCl, 5% NP-40, 0.5% SDS, 2.5% sodium deoxycholate; diluted to 1x and cOmplete, EDTA-free protein inhibitor cocktail (Roche) and RNasin ribonuclease inhibitor (Promega) added directly before use.

Par-Clip High-salt buffer (store at 4°C): 50 mM Tris-HCl (pH 7.4), 1 M NaCl, 1 mM EDTA, 1% NP-40, 0.1% SDS, 0.5% sodium deoxycholate

Par-Clip Wash buffer (store at 4°C): 20 mM Tris-HCl (pH 7.4), 10 mM $MgCl_2$, 0.2% Tween-20

Par-Clip PK adjustment buffer: 100 mM Tris-HCl (pH 7.4), 50 mM NaCl, 10 mM EDTA

Par-Clip PK urea buffer: 100 mM Tris-HCl (pH 7.4), 50 mM NaCl, 10 mM EDTA, 7 M urea

Par-Clip SDS sample buffer (store at 4°C): 50 mM Tris-HCl (pH 6.5), 100 mM dithiothreitol (DTT), 2% SDS

Frackelton buffer (store at 4°C): 10 mM Tris, 30 mM $Na_4P_2O_7$, 50 mM NaCl, 50 mM NaF, 1% Triton X-100; pH adjusted to 7.1

RIPA buffer: 50 mM Tris-HCl (pH 8), 150 mM NaCl, 0.1% SDS; added just before use: 0.5% sodium deoxycholate, 1% Triton X-100, 1 mM PMSF, protease/phosphatase inhibitor cocktail; pH adjusted to 7.5

TBS-T (Tris-buffered saline with Tween-20) buffer: 140 mM NaCl, 2.5 mM KCl, 25 mM Tris, 0.1% Tween-20, in ddH_2O; pH adjusted to 8.0

TAE (Tris-acetate-EDTA) (1l): 242g Tris, 0.5 M EDTA, 100ml Glacial acetic acid (EDTA and glacial acetic acid were added after Tris had been dissolved)

Towbin/Transfer buffer: 25 mM Tris, 192 mM glycine, 20% (v/v) methanol; pH adjusted to 8.3

SDS-PAGE Running buffer: 25 mM Tris, 192 mM glycine, 0.1% SDS

6.4 **Plasmids**

pGL2-TRE, containing a luciferase gene under a Tet-responsive P_{tight} promoter, was the basis for the vectors pGL2-TRE-IL1α, pGL2-TRE-Hprt and pGL2-TRE-Areg, carrying the 3'UTRs of *Il1a*, *Hprt* and *Areg* respectively. A detailed description of the creation of the last plasmid can be found under *6.5 pGL2-TRE-Areg reporter cloning*. The expression of the luciferase gene with varying 3'UTRs fused to its 3' end is dependent on the presence of the tet-controlled transactivator which is expressed form the pTet-On Advanced plasmid (Clontech). TTP was expressed from the CMV-TTP-Flag plasmid (Plasmid maps in Fig. 25). Additionally, the empty plasmid pcDNA 3.1 and the GFP-carrying plasmid Cop-GFP (where GFP is coupled to the CopA protein) were used.

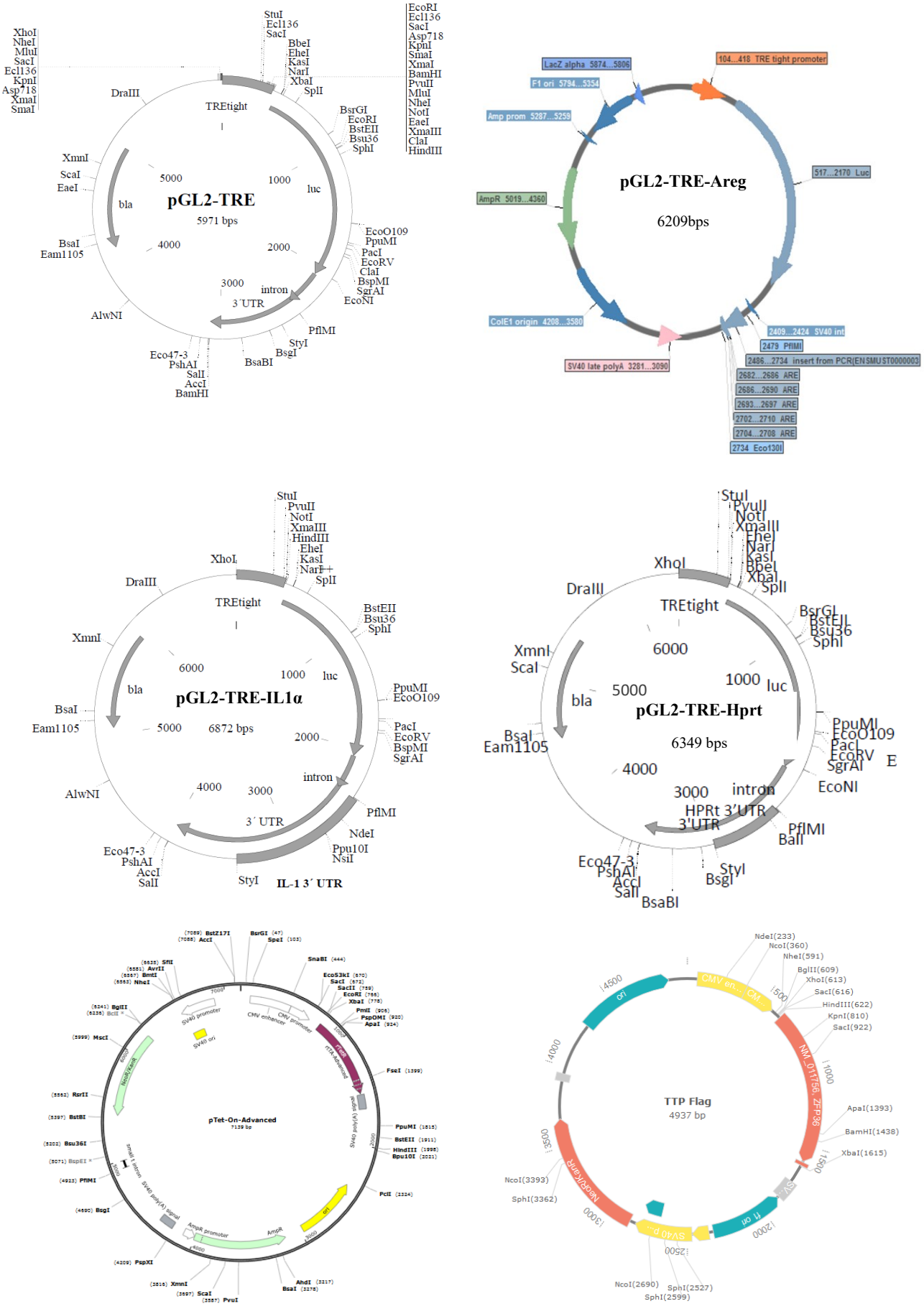

Fig. 25 Plasmid maps pGL2-TRE and its derivatives pGL2-TRE-IL1α, pGL2-TRE-Hprt and pGL2-TRE-Areg, as well as the transactivator plasmid pTet-On-Advanced and CMV-TTP-Flag (plasmid maps created with SnapGene and Serial Cloner).

6.5 **pGL2-TRE-Areg reporter cloning**

RNA was isolated from alveolar macrophages from $TTP^{\Delta M}$ mice stimulated with LPS for 3h using acidic phenol/chloroform (5:1, pH 4.5, Ambion) isolation. RNA was transcribed to cDNA. The 3'UTR of the Areg gene was amplified using 0.25µl Q5 High fidelity DNA polymerase (2000U/ml, NEB), 5µl 5x Q5 reaction buffer (NEB), 0.5µl 10nM dNTPs (ThermoFisher), 1.25µl each of 10µM *Areg*_3'UTR forward and reverse primer (Eurofins), 5µl 5x Q5 High GC Enhancer (NEB) and 2µl cDNA in a 25µl reaction yielding a 395bp product. PCR program: 98°C for 20s, 30x (98°C for 10s, 55°C for 20s, 72°C for 20s), 72°C for 2min, 4°C hold, on ARKTIK ThermoCycler (ThermoFisher). The band of the right size was cut from a 1% agarose gel and purified using Monarch DNA gel extraction kit (NEB). The restriction sites for the enzymes PflmI/Van91 (Fermentas) and StyI/Eco130I (ThermoFisher) were inserted using 30ng DNA and PflMI_*Areg*_3'UTR fw and StyI_*Areg*_3'UTR rv primers ordered from Eurofins with the same PCR program with an annealing temperature of 65.4°C.

The resulting fragment was digested using 1µl each of StyI and PflMI, 2µl FastDigest Green Buffer (10X) (ThermoFisher) and 2.3µg DNA in 30µl volume while the vector pGL2-TRE containing an Ampicillin resistance gene was digested using 0.5µl each of PfIMI and StyI, 2µl FastDigest Green Buffer (10X), and 3µg DNA in 20µl volume. The mixtures were incubated on 37°C for 30min after which the insert was isolated using Monarch PCR ad DNA Clean-up kit (NEB) and the vector was isolated from an agarose gel using the Monarch DNA gel extraction kit (NEB). The vector was then dephosphorylated by incubating at 37°C for 10min with 1µl FastAP Thermosensitive Alkaline Phosphatase (1U/µl, ThermoFisher) and 2µl reaction buffer in 20µl volume before deactivating the enzyme at 75°C for 5min. After purifying the vector, insert and vector were ligated using a vector : insert ration of 1:5 using 2µl 10x T4 ligase buffer and 0.2µl/1U T4 ligase (ThermoFisher) in 20µl volume by incubating overnight at 16°C before inactivating the enzyme at 65°C for 10min. 100µl $CaCl_2$-competent *E. coli* (DH10b) were transfected with 10µl of ligation mix by incubating on ice for 30min and then putting them at 42°C for 2min before adding 900µl LB medium (1L: 10g tryptone, 5g yeast extract, 10g NaCl, pH 7) and incubating for 1 hour at 37°C while slightly shaking. Then the bacteria were spun for 3min at 2841rcf and resuspended in 100µl of LB medium and plated on agar plates containing ampicillin (100µg/ml) which were put on 28°C overnight. Single colonies were picked and grown at 28°C before isolating the plasmid using a plasmid mini prep kit (Qiagen). The plasmid was sent to Eurofins for sequencing using *Luc_Areg* 1 and 2 primers.

Primers for reporter cloning	
*Areg*_3'UTR fw	CTTTGTCTCTGCCATCATCC
*Areg*_3'UTR rv	AAAAAAAGTTTAATGAGCTATAAA
PflMI_*Areg*_3'UTR fw	TTTTTCCAACCTATGGctgaggacaatgcagggtaa
StyI_*Areg*_3'UTR rv	GCGGCCCTTGGaaaaaaagtttaatgagcta
*Luc_Areg*_1	CGCCAGTCAAGTAACAACCG
*Luc_Areg*_2	TCCTTTGTGGTGTAAATAGC

6.6 Transfection

Unless otherwise stated, cells were transfected by first mixing Opti-MEM reduced serum media (ThermoFisher) and polyethylenimine (PEI) (3µl PEI per 1µg DNA) and then adding the mixture to plasmid mixes in Opti-MEM. Together DNA and PEI were incubated for 30min at room temperature and then added dropwise to the cells.

When cells were transfected with FuGENE (Promega), 3µl transfection reagent per µg DNA in Opti-MEM were used and the mixture incubated at room temperature for 15min before slowly adding it onto the cells.

Suspension method: Cells were resuspended in the transfection mix (containing PEI or FuGENE plus the DNA) and seeded onto 6cm dishes after 15min incubation time at room temperature.

6.7 RNA isolation

From tissue: One half of the lungs isolated from infected or uninfected mice was smashed using an ultrasonic tissue homogenizer (PolyTron PT2100, Kinematica) in 1ml QIAzol Lysis Reagent (Qiagen) and 500µl of the solution were used for RNA isolation as described below.

From cell culture: Cells were washed with cold PBS, scraped in QIAzol Lysis Reagent (6cm dishes: 500µl, 10cm dishes: 750 µl) and vortexed for 15 seconds. Chloroform was added (6cm dishes: 150µl, 10cm dishes: 200µl) and samples vortexed for 15 seconds before spinning them for 5min at 21 130rcf (max. speed) (Centrifuge 5424R, Eppendorf). The aqueous phase was transferred to a new Eppendorf tube and 1 volume isopropanol and 1/10 volume 4 M NaCl were added. Samples were mixed gently and incubated at room temperature for 10min before spinning at maximum speed for 30min at 4°C. The pellet was washed twice with 75% ethanol and resuspended in nuclease-free water.

6.8 DNase treatment and RNA precipitation

10µl of DNase I buffer (Roche), 1µl of RNasin (Promega) and 1µl DNase I (recombinant, Roche) were added to 5µg of RNA, filled up to 50µl with nuclease-free water and incubated at 37°C for 20min before adding 150µl nuclease-free water. An equal amount of acidic phenol-chloroform (5:1, pH 4.5, Ambion) was added, the solution was vortexed and spun for 10min at 15 871rcf at 4°C. An equal amount of

chloroform was added and after vortexing, the samples were again spun down for 10min at 16 363rcf, 4°C. The aqueous phase was transferred to new Eppendorf tubes and 20µl sodium acetate (3 M, pH 5.2), 1µl GlycoBlue (ThermoFisher) and 600µl of 96% ethanol were added before vortexing and incubating overnight at -20°C to allow precipitation. Samples were spun for 45min at 16 363rcf, 4°C, the supernatant was removed and the pellet was washed with 1ml cold 80% ethanol. The pellet was resuspended in nuclease-free water.

6.9 **cDNA synthesis**

RNA, and 1µl oligo d(T) primer or random hexamer primers (Eurofins) for RNA from PAR-CLIP were incubated at 70°C for 5min in a final volume of 11µl. 4µl 5x reaction buffer, 2µl 10nM dNTPs and 2µl nuclease-free water were added to each sample which were incubated at 37°C for 5min. 1µl of Mu-MLV Revert Aid transcriptase (200U/µl, ThermoFisher) or SuperScript IV reverse transcriptase (200U/µl, ThermoFisher) was added and samples were incubated at 42°C for one hour. The reaction was terminated by incubating at 70°C for 10min and all samples were diluted 1/10.

6.10 **Real-time quantitative PCR**

5µl cDNA, 4µl 5x HOT FIREPol® EvaGreen® qPCR Mix (Medibena), 0.075µl each of forward and reverse primer and 10.85µl nuclease-free water were used per reaction for a final reaction volume of 20µl. PCR program: 95°C for 15min, 40x (95°C for 15s, 60°C for 20s, 72°C for 20s), 95°C for 20s, 58°C for 15s, melt curve 58°C to 95°C in 0.5°C steps for 5s, on CFX96 Touch Real-time PCR detection system (BioRad).

qPCR primers	**Organism**	**Sequence (5'-3')**
Hprt FV	Human	TGTGTGCTCAAGGGGGGC
Hprt RV	Human	CGTGGGGTCCTTTTCACC
ADAMTS1 FW	Human	CAGCCCAAGGTTGTAGATGGT
ADAMTS1 RV	Human	CCTCTGGTTCCGCTGTTTCA
JUN FW	Human	GCCAGGTCGGCAGTATAGTC
JUN RV	Human	GGACTCTGCCACTTGTCTCC
Hprt FW	Mouse	GCAGTCCCAGCGTCGTGAT
Hprt RV	Mouse	CAGGCAAGTCTTTCAGTCCTGTC
Il1a FW	Mouse	CCATCCAACCCAGATCAGCA
Il1a RV	Mouse	GTTTCTGGCAACTCCTTCAGC
Il1b FW	Mouse	AGATGAAGGGCTGCTTCCAAA
Il1b RV	Mouse	AATGGGAACGTCACACACCA
IL6 FW	Mouse	ATGGATGCTACCAAACTGGAT
IL6 RV	Mouse	TGAAGGACTCTGGCTTTGTCT
Cxcl1 FW	Mouse	TGCACCCAAACCGAAGTCATAG
Cxcl1 RV	Mouse	TTGTATAGTGTTGTCAGAAGCCAGC
Cxcl2 FW	Mouse	GCCCAGACAGAAGTCATAG
Cxcl2 RV	Mouse	GTCAGTTAGCCTTGCCTT
IFNb FW	Mouse	TCAGAATGAGTGGTGGTTGC
IFNb RV	Mouse	GACCTTTCAAATGCAGTAGATTCA
TNF FW	Mouse	GATCGGTCCCCAAAGGGATG
TNF RV	Mouse	CACTTGGTGGTTTGCTACGAC

6.11 **mRNA stability assay**

500 000 HEK 293T cells per well were seeded in 6 well plates in DMEM+10% FCS without Pen/Strep. Cells were transfected with a total of 1µg DNA per well in ratios of TTP : Tet-on : Reporter = 1 : 1.3 : 4 or 1 : 5 : 15 using Opti-Mem and PEI (3µl per 1µg DNA). After six hours reporter expression was induced with doxycycline (1µg/ml). After 16 hours, transcription was stopped with actinomycin D (5µg/ml) and cells harvested in 500µl QIAzol Lysis reagent after 0min, 45min and 90min. RNA was isolated. After qPCR, the level of mRNA at each timepoint was represented as percentage of its level at timepoint 0.

6.12 **PAR-CLIP**

10 million cells were seeded on 15cm dishes. Cells were transfected 6 hours before 4-thiouridine (4sU) (100µM) and doxycycline (1µg/ml) were added for 16 hours. Cells were washed with PBS, which was removed completely before plates were irradiated without lids in a Stratalinker 2400 (Stratagene) (dose: 0.15J/cm^2, 365nm). Cells were scraped into PBS and pelleted at 700rcf for 5min, 4°C. 50µl of Pierce Protein A/G magnetic beads (ThermoFisher) per sample were washed twice in 1x lysis buffer using a magnetic rack before resuspending them in their original volume in rabbit anti-TTP serum or pre-immune serum as negative control. The beads were incubated with the antibody for 45min at room temperature while rotating and then washed trice with 900µl 1x lysis buffer. The cell pellets were resuspended in 1x lysis buffer (3x pellet volume) with 1µl RNasin ribonuclease inhibitor (Promega) and incubated on ice for 10min. 10µl of DNase I (10U/µl, Roche) were added to the cell lysates and incubated for 20min at 37°C. Then the lysates were spun at 21130rcf for 20min, 4°C and the supernatant was collected. 1/10 of the volume was taken for the input and the remainder was added to the antibody-coated beads. The mixture was rotated overnight at 4°C after which the supernatant was discarded, and the beads washed once with 900µl high salt buffer and trice with 900µl buffer. RNA-protein complexes were released from the beads by incubating at 70°C for 10min in 100µl PAR-CLIP SDS sample buffer. 100µl PK adjustment buffer were added to the supernatant and to the input. 10µl proteinase K solution (Roche) were added to each sample and incubated for 30min at 37°C before adding 200µl PK urea buffer and incubating again for 30min at 37°C. Afterwards, 400µl acidic phenol/chloroform were added to the solution and vortexed vigorously. Samples were spun at 15871rcf for 10min, 4°C and the aqueous phase was transferred to a new Eppendorf tube where 1µl GlycoBlue, 1:10 3 M sodium acetate pH 5.5 and 1ml 96% ethanol (undenatured) were added. RNA was precipitated at -20°C overnight and collected by spinning at 21130rcf for 30min at 4°C. The pellet was washed in 80% ethanol and resuspended in nuclease-free water.

Analysis of qPCR data: the mean starting quantity (SQ) of each sample was divided by the mean SQ of the corresponding input. This was again divided by the input SQ and multiplied by 100 to represent the level of target gene in the pull-down as percentage of its input.

6.13 **ELISA**

According to manufacturer's protocol (R&D systems). In short: the wells were incubated with capture antibody overnight, then blocked with Reagent diluent containing BSA for 1h. 50µl of sample were added to the antibody for 2h before incubating with 50µl detection antibody for 2h. 100µl of streptavidin-HRP was added to each well and incubated for 20min in the dark. Then 100µl substate solution were added to each well and also incubated for 20min in the dark, before stopping the reaction by adding 50µl stop solution. Analysis with a plate reader at 450nm, wavelength correction 540 or 570nm). The amount of total protein was measured using Pierce BCA protein assay kit (ThermoFisher) and the concentration of target protein expressed as pg/mg/ml total protein.

6.14 **SDS-PAGE and western blot**

Cells were scraped in 150µl RIPA buffer and incubated on ice for 5min, spun for 5min at 21130rcf and 50µg of protein were loaded on a 5% stacking (1.35ml ddH_2O, 150µl Acrylamid-Bis solution 50%, 0.5ml 0.5 M Tris (pH 6.8), 20µl 10% SDS, 6µl APS, 4µl TEMED) and 10% resolving gel (2.2ml ddH_2O, 0.8ml Acrylamid-Bis solution 50%, 1ml 1.5M Tris (ph 8.8), 40µl 10% SDS, 12µl 20% APS, 8µl TEMED) and run at constant 20mA. Protein was transferred to a nitrocellulose membrane (Sigma-Aldrich) using the Trans-blot Turbo Transfer System (Biorad), a semi-dry transfer, for 15min using Towbin buffer. The membrane was blocked with 10% milk in TBS-T and incubated with anti-TTP K2 ("housemade" antibody, 1:2500 in TBS-T and 1% BSA, rabbit) antibody overnight at 4°C. Secondary anti-rabbit antibody (1:4000, 5% milk in TBS-T) was added for 1 hour and the membrane analysed using the ChemiDoc Touch Imaging system (Biorad) using SuperSignal West Pico PLUS Chemiluminescence substrate (ThermoFisher).

6.15 **Cultivation of *S. pneumoniae* (ATCC 6303)**

Bacteria were streaked out from frozen stock on Columbia agar plates with Sheep blood (Oxoid) which were incubated at 37°C. Two to three colonies were picked and inoculated in THY medium (for 1l: 30g Todd Hewitt broth, 2g yeast extract)**.** The bacteria were five times serially diluted 1:100 and incubated overnight at 37°C (non-shaking). The least dense culture (optical density measured at 630nm) was diluted 1:10 and incubated at 37°C until OD_{630} 0.4-0.6. Bacteria were spun at 1000rcf for 15min at 4°C in centrifuge 5810R (Eppendorf) and washed in PBS.

6.16 **Cultivation of *S. pyogenes* (EC 700)**

An overnight culture in 5ml THY was grown from frozen stock at 37°C (non-shaking) and then diluted 1:15 in THY and grown until OD_{600} 0.4. The bacteria were pelleted by spinning at 6000rcf for 8min at 4°C and washed in PBS.

6.17 **Staining and heat-killing of bacteria**

CFSE staining of *S. pneumoniae* and *S. pyogenes*: Bacteria were resuspended in 2ml PBS and stained with CFSE (1:1000, ThermoFisher) for 20min, gently shaking at 37°C. Tubes were protected from light. The bacteria were washed trice with PBS and resuspended in 2ml PBS. Bacteria were killed by incubating them at 65°C (*S. pneumoniae*) or 70°C (*S. pyogenes*) for 40min after which they were streaked out on blood agar plates to check if all bacteria were dead.

pHrodo staining of *S. pneumoniae*: Heat-killed bacteria were stained with pHrodo (ThermoFisher) (1µM – 500µM) by incubating at 37°C for 30min while mildly shaking.

Counting CFUs: Before heat-killing bacteria, an aliquot was diluted serially 1:100 to 10^{-8} and the Miles and Misra method[178] was used to count CFUs. Thereby five drops of 10µl of dilutions 10^{-5} to 10^{-8} were dropped onto two blood agar plates and the mean number of colonies of both plates per concentration was calculated before the mean number of colonies of the different concentrations was calculated.

6.18 **Killing assay**

BMDMs were seeded in untreated 12 well plates and infected with live *S. pneumoniae,* MOI (multiplicity of infection) 25. The plates were spun for 5min at 1000rcf and incubated at 37°C for one hour after which the medium (DMEM without serum or antibiotics) was removed and the wells were washed trice with ice-cold sterile PBS to remove extra-cellular bacteria. Untransfected cells and cells for timepoint 0 were lysed in 100µl filtered 0.1% saponin in PBS for 5min, then 900µl PBS were added to dilute the saponin. Fresh medium with 90µl gentamycin in 30ml medium to kill external bacteria was added to the other wells, which were incubated for 1, 2 and 3 hours at 37°C, after which cells were washed with PBS and lysed the same way. The lysates were serially diluted from -1 to -4 and 50µl of each were plated in 10µl drops on blood agar plates. Bacteria were plated to count their actual CFUs.

6.19 **Phagocytosis assays**

Cells were seeded in plates (tissue culture treated for RAW macrophages and all experiments using the plate reader, untreated for BMDMs and AMs) and incubated with heat-killed bacteria or 1µm diameter fluorescent biotin-labelled beads (FluoSpheres™ Biotin-Labeled Microspheres, yellow-green fluorescent (505/515), ThermoFisher) for 1 or 2 hours respectively. For the no phagocytosis control, plates were stored at 4°C for one hour before adding of bacteria/beads and during the incubation

period. After adding the bacteria/beads the plates were centrifuged at 500rcf for 5min to spin the particles onto the cells. Then the cells were washed two times with PBS to remove external bacteria.

For LPS stimulation, 10ng/ml LPS were added to the medium for 3h, or 1ng/ml LPS overnight.

6.20 **FACS staining and analysis**

Cells were harvested in 250µl PBS and transferred into a 96 V-shaped well plate. In the case of non-adherend cells (BMDMs of the 4°C no phagocytosis control) the whole well content was transferred to falcons and the washing steps performed by centrifugation at 300rcf for 5min. Cells in 96 well plate were spun down at 300rcf for 5min, resuspended in 200µl 1:2000 fixable viability dye in PBS and incubated at room temperature for 30min in the dark. Cells were spun down and resuspended in 25µl Fcγ block (BD) in FACS buffer (PBS with 0.1% NaN_3, 0.5% BSA) when antibody staining was performed. Cells were incubated for 15min at room temperature in the dark, the wells were filled up to 200µl and cells spun down before they were resuspended in FACS buffer with antibodies (all antibodies were used at a dilution of 1:100) and incubated at 4°C for 30min in the dark. Wells were filled up to 200µl and spun down, then washed once in FACS buffer and cells transferred to FACS tubes by passing the suspension through a tissue filter. Cells were analysed with the LSR Fortessa Flow cytometer (BD).

Life/dead staining for flow cytometry: fixable viability dye (efluor780: APC-Cy7 (Cat. # 65-0865-14) and efluor506: BV510 (Cat. # 65-0866-14), eBioscience)

Antibodies for flow cytometry:

Antigen	Fluorochrome	Clone number	Catalogue number	Company
Streptavidin (binding Biotin)	PE	-	405203	BioLegend
F4/80	APC	BM8	17-4801-82	eBioscience
CD11c	APC	HL3	550261	BD Bioscience
CD11c	BV421	N418	117330	BioLegend
CD11b	PerCP-Cy5.5	M1/70	45-0112-82	eBioscience
CD11b	PECy7	M1/70	25-0112-82	Invitrogen
SigLec-F	BV421	E50-2440	565934	BD Horizon

6.21 **Analysis of phagocytosis using a plate reader**

Cells were stained with Streptavidin-PE (1:100) for 10min at room temperature, washed twice with PBS, wells filled with 200µl PBS and then analysed using the Synergy H1 microplate reader from Biotek using these filter settings: excitation: 488nm, emission: 518nm to detect the bead signal (corresponds to FITC signal); excitation: 550nm, emission: 580nm to detect Streptavidin-PE signal (external beads). Signal was read without plate lid from the top, gain: 100. Phagocytic cells were represented as FITC signal minus PE signal.

6.22 **Infection of mice**

Mice were infected intra-nasally with live *S. pneumoniae* (approximately 10^4 bacteria in 30µl suspension). Bacterial CFUs were counted to determine actual bacterial concentration. After 72h mice were sacrificed and lungs were harvested for histology or used for RNA isolation.

6.23 **Tissue slice preparation**

Mice were sacrificed using anaesthesia (10ml: 0.5ml Sedaxylan (20mg/ml, Covetrus) and 1ml Ketamidor (100mg/ml, Richter Pharma) in 0.9% NaCl) or cervical dislocation. The trachea and lung were exposed and the lungs inflated with approximately 1ml 4% paraformaldehyde (PFA) in PBS. The trachea was tied off with thread and the lungs placed into tissue cassettes which were kept in 4% PFA solution overnight at 4°C. The PFA was exchanged for 70% ethanol in the morning and again 6 hours later, after which the samples were dehydrated in a dehydration machine (Shandon Excelsior, ThermoFisher):

1. 70% ethanol – 1h
2. 90% ethanol – 1h
3. 96% ethanol – 1h
4. 100% ethanol – 1h
5. 100% ethanol – 1h
6. 100% ethanol – 1h
7. Xylol – 1h
8. Xylol – 1h
9. Xylol – 1h
10. Paraffin – 1h 20 min
11. Paraffin – 1h 20 min
12. Paraffin – 1h 20 min

The lungs were embedded in paraffin wax on a HistoStar (ThermoFisher) and 3µm tissue slices were cut from the blocks using the Leica RM2255 microtome (Leica Biosystems).

6.24 **Haematoxylin/Eosin staining**

Tissue slides were H/E stained in a Gemini AS machine (ThermoFisher): Tissue slides were warmed at 60°C for 2min and then rehydrated and stained in the machine according to the following protocol:

1. Xylol substitute Histolab Clear (HistoLab) – 10 min
2. Xylol substitute Histolab Clear (HistoLab) – 10 min
3. 96% ethanol – 30 sec
4. 96% ethanol – 30 sec
5. 90% ethanol – 30 sec
6. 70% ethanol – 30 sec
7. Rinse with running tap water – 1 min
8. Nuclear stain with Papanicolaou's solution 1a Harris' haematoxylin solution (Sigma-Aldrich) – 5 min
9. Bluing with running tap water – 30s
10. Differentiate with 0,37% HCl-ethanol – 2 sec
11. Bluing with running tap water – 10 min
12. 70% ethanol – 2 min
13. 80% ethanol – 2 min
14. Eosin Y, alcoholic (0.5 % (w/v) in acidified ethanol, Sigma-Aldrich) – 1 min
15. 90% ethanol – 30 sec
16. 90% ethanol – 30 sec
17. 96% ethanol –1 min
18. 96% ethanol – 1 min
19. n-Butylacetat – 2 min
20. n-Butylacetat – 3 min

Afterwards, slides were mounted using Eukitt quick hardening mounting medium (Sigma-Aldrich) and covered with a cover slip.

7 References

1. Hammond SM, Boettcher S, Caudy AA, Kobayashi R, Hannon GJ. Argonaute2, a link between genetic and biochemical analyses of RNAi. *Science (80-)*. 2001;293(5532):1146-1150. doi:10.1126/science.1064023

2. Schwarz DS, Hutvágner G, Haley B, Zamore PD. Evidence that siRNAs function as guides, not primers, in the Drosophila and human RNAi pathways. *Mol Cell*. 2002;10(3):537-548. doi:10.1016/S1097-2765(02)00651-2

3. Ambros V. The functions of animal microRNAs. *Nature*. 2004;431(7006):350-355. doi:10.1038/nature02871

4. Agrawal N, Dasaradhi PVN, Mohmmed A, Malhotra P, Bhatnagar RK, Mukherjee SK. RNA Interference: Biology, Mechanism, and Applications. *Microbiol Mol Biol Rev*. 2003;67(4):657-685. doi:10.1128/mmbr.67.4.657-685.2003

5. Bernstein P, Peltz SW, Ross J. The poly(A)-poly(A)-binding protein complex is a major determinant of mRNA stability in vitro. *Mol Cell Biol*. 1989;9(2):659-670. doi:10.1128/mcb.9.2.659

6. Kahvejian A, Svitkin Y V., Sukarieh R, M'Boutchou MN, Sonenberg N. Mammalian poly(A)-binding protein is a eukaryotic translation initiation factor, which acts via multiple mechanisms. *Genes Dev*. 2005;19(1):104-113. doi:10.1101/gad.1262905

7. Tucker M, Valencia-Sanchez MA, Staples RR, Chen J, Denis CL, Parker R. The transcription factor associated Ccr4 and Caf1 proteins are components of the major cytoplasmic mRNA deadenylase in Saccharomyces cerevisiae. *Cell*. 2001;104(3):377-386. doi:10.1016/S0092-8674(01)00225-2

8. Uchida N, Hoshino SI, Katada T. Identification of a Human Cytoplasmic Poly(A) Nuclease Complex Stimulated by Poly(A)-binding Protein. *J Biol Chem*. 2004;279(2):1383-1391. doi:10.1074/jbc.M309125200

9. Dehlin E, Wormington M, GKö rner C, Wahle E, Anderson J. *Cap-Dependent Deadenylation of MRNA*. Vol 19.; 2000.

10. van Dijk E, Cougot N, Meyer S, Babajko S, Wahle E, Séraphin B. Human Dcp2: a catalytically active mRNA decapping enzyme located in specific cytoplasmic structures. *EMBO J*. 2002;21(24):6915-6924. doi:10.1093/emboj/cdf678

11. Jones CI, Zabolotskaya MV, Newbury SF. The 5′ → 3′ exoribonuclease XRN1/Pacman and its functions in cellular processes and development. *Wiley Interdiscip Rev RNA*. 2012;3(4):455-468. doi:10.1002/wrna.1109

12. Van Hoof A, Parker R. The exosome: A proteasome for RNA? *Cell*. 1999;99(4):347-350. doi:10.1016/S0092-8674(00)81520-2

13. Das S, Sarkar D, Das B. The interplay between transcription and mRNA degradation in saccharomyces cerevisiae. *Microb Cell*. 2017;4(7):212-228. doi:10.15698/mic2017.07.580

14. Furuichi Y, LaFiandra A, Shatkin AJ. 5′-Terminal structure and mRNA stability. *Nature*. 1977;266(5599):235-239. doi:10.1038/266235a0

15. Shimotohno K, Kodama Y, Hashimoto J, Miura KI. Importance of 5′-terminal blocking structure to stabilize mRNA in eukaryotic protein synthesis. *Proc Natl Acad Sci U S A*. 1977;74(7):2734-2738. doi:10.1073/pnas.74.7.2734

16. Aharon T, Schneider RJ. Selective destabilization of short-lived mRNAs with the granulocyte-macrophage colony-stimulating factor AU-rich 3′ noncoding region is mediated by a cotranslational mechanism. *Mol Cell Biol*. 1993;13(3):1971-1980. doi:10.1128/mcb.13.3.1971

17. Halees AS, Hitti E, Al-Saif M, et al. Global assessment of GU-rich regulatory content and function in the human transcriptome. *RNA Biol*. 2011;8(4):681. doi:10.4161/rna.8.4.16283

18. Vlasova IA, Tahoe NM, Fan D, et al. Conserved GU-Rich Elements Mediate mRNA Decay by Binding to CUG-Binding Protein 1. *Mol Cell*. 2008;29(2):263-270. doi:10.1016/j.molcel.2007.11.024

19. Barron VA, Zhu H, Hinman MN, Ladd AN, Lou H. The neurofibromatosis type I pre-mRNA is a novel target of CELF protein-mediated splicing regulation. *Nucleic Acids Res*. 2009;38(1):253-264. doi:10.1093/nar/gkp766

20. Moraes KCM, Wilusz CJ, Wilusz J. CUG-BP binds to RNA substrates and recruits PARN deadenylase. *RNA*. 2006;12(6):1084-1091. doi:10.1261/rna.59606

21. Zhang L, Lee JE, Wilusz J, Wilusz CJ. The RNA-binding protein CUGBP1 regulates stability of tumor necrosis factor mRNA in muscle cells: Implications for myotonic dystrophy. *J Biol Chem*. 2008;283(33):22457-22463. doi:10.1074/jbc.M802803200

22. Tu Y, Wu X, Yu F, et al. Tristetraprolin-RNA interaction map reveals a novel TTP-RelB regulatory network for innate immunity gene expression. *Mol Immunol*. 2020;121:59-71. doi:10.1016/j.molimm.2020.02.004

23. Bakheet T, Hitti E, Al-Saif M, Moghrabi WN, Khabar KSA. The AU-rich element landscape across human transcriptome reveals a large proportion in introns and regulation by ELAVL1/HuR. *Biochim Biophys Acta - Gene Regul Mech*. 2018;1861(2):167-177. doi:10.1016/j.bbagrm.2017.12.006

24. Shaw G, Kamen R. A conserved AU sequence from the 3' untranslated region of GM-CSF mRNA mediates selective mRNA degradation. *Cell*. 1986;46(5):659-667. doi:10.1016/0092-8674(86)90341-7

25. Chen CYA, Shyu A Bin. AU-rich elements: characterization and importance in mRNA degradation. *Trends Biochem Sci*. 1995;20(11):465-470. doi:10.1016/S0968-0004(00)89102-1

26. Barreau C, Paillard L, Osborne HB. AU-rich elements and associated factors: Are there unifying principles? *Nucleic Acids Res*. 2005;33(22):7138-7150. doi:10.1093/nar/gki1012

27. Gratacós FM, Brewer G. The role of AUF1 in regulated mRNA decay. *Wiley Interdiscip Rev RNA*. 2010;1(3):457-473. doi:10.1002/wrna.26

28. Chen CYA, Xu N, Zhu W, Shyu A Bin. Functional dissection of hnRNP D suggests that nuclear import is required before hnRNP D can modulate mRNA turnover in the cytoplasm. *RNA*. 2004;10(4):669-680. doi:10.1261/rna.5269304

29. Wilson GM, Lu J, Sutphen K, et al. Phosphorylation of p40AUF1 regulates binding to A + U-rich mRNA-destabilizing elements and protein-induced changes in ribonucleoprotein structure. *J Biol Chem*. 2003;278(35):33039-33048. doi:10.1074/jbc.M305775200

30. Sagliocco F, Laloo B, Cosson B, et al. The ARE-associated factor AUF1 binds poly(A) in vitro in competition with PABP. *Biochem J*. 2006;400(2):337-347. doi:10.1042/BJ20060328

31. Chen CY, Gherzi R, Ong SE, et al. AU binding proteins recruit the exosome to degrade ARE-containing mRNAs. *Cell*. 2001;107(4):451-464. doi:10.1016/S0092-8674(01)00578-5

32. Brewer G. An A + U-rich element RNA-binding factor regulates c-myc mRNA stability in vitro. *Mol Cell Biol*. 1991;11(5):2460-2466. doi:10.1128/mcb.11.5.2460

33. Xu N, Chen C-YA, Shyu A-B. Versatile Role for hnRNP D Isoforms in the Differential Regulation of Cytoplasmic mRNA Turnover. *Mol Cell Biol*. 2001;21(20):6960-6971. doi:10.1128/mcb.21.20.6960-6971.2001

34. Lafon I, Carballès F, Brewer G, Poiret M, Morello D. Developmental expression of AUF1 and HuR, two c-myc mRNA binding proteins. *Oncogene*. 1998;16(26):3413-3421. doi:10.1038/sj.onc.1201895

35. Raineri I, Wegmueller D, Gross B, Certa U, Moroni C. Roles of AUF1 isoforms, HuR and BRF1 in ARE-dependent mRNA turnover studied by RNA interference. *Nucleic Acids Res*. 2004;32(4):1279-1288. doi:10.1093/nar/gkh282

36. Sarkar B, Xi Q, He C, Schneider RJ. Selective Degradation of AU-Rich mRNAs Promoted by the p37 AUF1 Protein Isoform. *Mol Cell Biol*. 2003;23(18):6685-6693. doi:10.1128/mcb.23.18.6685-6693.2003

37. Wilson GM, Lu J, Sutphen K, Sun Y, Huynh Y, Brewer G. Regulation of A + U-rich element-directed mRNA turnover involving reversible phosphorylation of AUF1. *J Biol Chem*. 2003;278(35):33029-33038. doi:10.1074/jbc.M305772200

38. Alspach E, Flanagan KC, Luo X, et al. P38MAPK plays a crucial role in stromal-mediated tumorigenesis. *Cancer Discov*. 2014;4(6):716-729. doi:10.1158/2159-8290.CD-13-0743

39. Li M-L, Defren J, Brewer G. Hsp27 and F-Box Protein -TrCP Promote Degradation of mRNA Decay Factor AUF1. *Mol Cell Biol*. 2013;33(11):2315-2326. doi:10.1128/mcb.00931-12

40. Kedar VP, Zucconi BE, Wilson GM, Blackshear PJ. Direct binding of specific AUF1 isoforms to tandem zinc finger domains of tristetraprolin (TTP) family proteins. *J Biol Chem*. 2012;287(8):5459-5471. doi:10.1074/jbc.M111.312652

41. Fan XC, Steitz JA. Overexpression of HuR, a nuclear-cytoplasmic shuttling protein, increases the in vivo stability of ARE-containing mRNAs. *EMBO J*. 1998;17(12):3448-3460. doi:10.1093/emboj/17.12.3448

42. Lebedeva S, Jens M, Theil K, et al. Transcriptome-wide Analysis of Regulatory Interactions of the RNA-Binding Protein HuR. *Mol Cell*. 2011;43(3):340-352. doi:10.1016/j.molcel.2011.06.008

43. Barnhart MD, Moon SL, Emch AW, Wilusz CJ, Wilusz J. Changes in Cellular mRNA Stability, Splicing, and Polyadenylation through HuR Protein Sequestration by a Cytoplasmic RNA Virus. *Cell Rep*. 2013;5(4):909-917. doi:10.1016/j.celrep.2013.10.012

44. Diaz-Muñoz MD, Bell SE, Fairfax K, et al. The RNA-binding protein HuR is essential for the B cell antibody response. *Nat Immunol*. 2015;16(4):415-425. doi:10.1038/ni.3115

45. Dai W, Zhang G, Makeyev E V. RNA-binding protein HuR autoregulates its expression by promoting alternative polyadenylation site usage. *Nucleic Acids Res*. 2012;40(2):787-800. doi:10.1093/nar/gkr783

46. Akaike Y, Masuda K, Kuwano Y, et al. HuR Regulates Alternative Splicing of the TRA2 Gene in Human Colon Cancer Cells under Oxidative Stress. *Mol Cell Biol*. 2014;34(15):2857-2873. doi:10.1128/mcb.00333-14

47. Doller A, Akool E-S, Huwiler A, et al. Posttranslational Modification of the AU-Rich Element Binding Protein HuR by Protein Kinase Cδ Elicits Angiotensin II-Induced Stabilization and Nuclear Export of Cyclooxygenase 2 mRNA. *Mol Cell Biol*. 2008;28(8):2608-2625. doi:10.1128/mcb.01530-07

48. Slone S, Anthony SR, Wu X, et al. Activation of HuR downstream of p38 MAPK promotes cardiomyocyte hypertrophy. *Cell Signal*. 2016;28(11):1735-1741. doi:10.1016/j.cellsig.2016.08.005

49. Farooq F, Balabanian S, Liu X, Holcik M, MacKenzie A. p38 Mitogen-activated protein kinase stabilizes SMN mRNA through RNA binding protein HuR. *Hum Mol Genet*. 2009;18(21):4035-4045. doi:10.1093/hmg/ddp352

50. Chen J, Martindale JL, Abdelmohsen K, et al. RNA-Binding Protein HuR Promotes Th17 Cell Differentiation and Can Be Targeted to Reduce Autoimmune Neuroinflammation. *J Immunol*. 2020;204(8):2076-2087. doi:10.4049/jimmunol.1900769

51. Chen J, Adamiak W, Huang G, Atasoy U, Rostami A, Yu S. Interaction of RNA-binding protein HuR and miR-466i regulates GM-CSF expression. *Sci Rep*. 2017;7(1). doi:10.1038/s41598-017-17371-5

52. Dean JLE, Wait R, Mahtani KR, Sully G, Clark AR, Saklatvala J. The 3' Untranslated Region of Tumor Necrosis Factor Alpha mRNA Is a Target of the mRNA-Stabilizing Factor HuR. *Mol Cell Biol*. 2001;21(3):721-730. doi:10.1128/mcb.21.3.721-730.2001

53. Techasintana P, Ellis JS, Glascock J, et al. The RNA-Binding Protein HuR Posttranscriptionally Regulates IL-2 Homeostasis and CD4 + Th2 Differentiation . *ImmunoHorizons*. 2017;1(6):109-123. doi:10.4049/immunohorizons.1700017

54. Tiedje C, Ronkina N, Tehrani M, et al. The p38/MK2-Driven Exchange between Tristetraprolin and HuR Regulates AU-Rich Element-Dependent Translation. *PLoS Genet*. 2012;8(9). doi:10.1371/journal.pgen.1002977

55. Wang W, Caldwell MC, Lin S, Furneaux H, Gorospe M. HuR regulates cyclin A and cyclin B1 mRNA stability during cell proliferation. *EMBO J*. 2000;19(10):2340-2350. doi:10.1093/emboj/19.10.2340

56. Bolognani F, Gallani AI, Sokol L, Baskin DS, Meisner-Kober N. MRNA stability alterations mediated by HuR are necessary to sustain the fast growth of glioma cells. *J Neurooncol*. 2012;106(3):531-542. doi:10.1007/s11060-011-0707-1

57. Wang W, Yang X, Cristofalo VJ, Holbrook NJ, Gorospe M. Loss of HuR Is Linked to Reduced Expression of Proliferative Genes during Replicative Senescence. *Mol Cell Biol*. 2001;21(17):5889-5898. doi:10.1128/mcb.21.17.5889-5898.2001

58. Pandiri I, Chen Y, Joe Y, et al. Tristetraprolin mediates the anti-proliferative effects of metformin in breast cancer cells. *Breast Cancer Res Treat*. 2016;156(1):57-64. doi:10.1007/s10549-016-3742-y

59. Deng K, Wang H, Shan T, et al. Tristetraprolin inhibits gastric cancer progression through suppression of IL-33. *Sci Rep*. 2016;6(1):1-14. doi:10.1038/srep24505

60. Lu YC, Chang SH, Hafner M, et al. ELAVL1 Modulates Transcriptome-wide miRNA Binding in Murine Macrophages. *Cell Rep*. 2014;9(6):2330-2343. doi:10.1016/j.celrep.2014.11.030

61. Hyeon HK, Kuwano Y, Srikantan S, Eun KL, Martindale JL, Gorospe M. HuR recruits let-7/RISC to repress c-Myc expression. *Genes Dev*. 2009;23(15):1743-1748. doi:10.1101/gad.1812509

62. Katsanou V, Papadaki O, Milatos S, et al. HuR as a negative posttranscriptional modulator in inflammation. *Mol Cell*. 2005;19(6):777-789. doi:10.1016/j.molcel.2005.08.007

63. Gherzi R, Chen CY, Ramos A, Briata P. KSRP Controls Pleiotropic Cellular Functions. *Semin Cell Dev Biol*. 2014;34:2-8. doi:10.1016/j.semcdb.2014.05.004

64. Winzen R, Thakur BK, Dittrich-Breiholz O, et al. Functional Analysis of KSRP Interaction with the AU-Rich Element of Interleukin-8 and Identification of Inflammatory mRNA Targets. *Mol Cell Biol*. 2007;27(23):8388-8400. doi:10.1128/mcb.01493-07

65. Li X, Lin WJ, Chen CY, et al. KSRP: A checkpoint for inflammatory cytokine production in astrocytes. *Glia*. 2012;60(11):1773-1784. doi:10.1002/glia.22396

66. Gherzi R, Lee KY, Briata P, et al. A KH domain RNA binding protein, KSRP, promotes ARE-directed mRNA turnover by recruiting the degradation machinery. *Mol Cell*. 2004;14(5):571-583. doi:10.1016/j.molcel.2004.05.002

67. R K, L S, K S, et al. The RNA-Binding Protein KSRP Modulates Cytokine Expression of CD4 + T Cells. *J Immunol Res*. 2019;2019. doi:10.1155/2019/4726532

68. Lin W-J, Zheng X, Lin C-C, et al. Posttranscriptional Control of Type I Interferon Genes by KSRP in the Innate Immune Response against Viral Infection. *Mol Cell Biol*. 2011;31(16):3196-3207. doi:10.1128/mcb.05073-11

69. Zhao H, Wang X, Yi P, et al. KSRP specifies monocytic and granulocytic differentiation through regulating miR-129

biogenesis and RUNX1 expression. *Nat Commun*. 2017;8(1):1-19. doi:10.1038/s41467-017-01425-3

70. Fujimoto T, Anderson K, Jacobsen SEW, Nishikawa SI, Nerlov C. Cdk6 blocks myeloid differentiation by interfering with Runx1 DNA binding and Runx1-C/EBPα interaction. *EMBO J*. 2007;26(9):2361-2370. doi:10.1038/sj.emboj.7601675

71. Linker K, Pautz A, Fechir M, Hubrich T, Greeve J, Kleinert H. Involvement of KSRP in the post-transcriptional regulation of human iNOS expression-complex interplay of KSRP with TTP and HuR. *Nucleic Acids Res*. 2005;33(15):4813-4827. doi:10.1093/nar/gki797

72. Briata P, Forcales SV, Ponassi M, et al. p38-Dependent phosphorylation of the mRNA decay-promoting factor KSRP controls the stability of select myogenic transcripts. *Mol Cell*. 2005;20(6):891-903. doi:10.1016/j.molcel.2005.10.021

73. Lai WS, Carballo E, Thorn JM, Kennington EA, Blackshear PJ. Interactions of CCCH zinc finger proteins with mRNA. Binding of tristetraprolin-related zinc finger proteins to AU-rich elements and destabilization of mRNA. *J Biol Chem*. 2000;275(23):17827-17837. doi:10.1074/jbc.M001696200

74. Blackshear PJ, Phillips RS, Ghosh S, Ramos SVB, Richfield EK, Lai WS. Zfp36l3, a Rodent X Chromosome Gene Encoding a Placenta-Specific Member of the Tristetraprolin Family of CCCH Tandem Zinc Finger Proteins. *Biol Reprod*. 2005;73(2):297-307. doi:10.1095/biolreprod.105.040527

75. Cao H, Tuttle JS, Blackshear PJ. Immunological characterization of tristetraprolin as a low abundance, inducible, stable cytosolic protein. *J Biol Chem*. 2004;279(20):21489-21499. doi:10.1074/jbc.M400900200

76. Sedlyarov V, Fallmann J, Ebner F, et al. Tristetraprolin binding site atlas in the macrophage transcriptome reveals a switch for inflammation resolution. *Mol Syst Biol*. 2016;12(5):868. doi:10.15252/msb.20156628

77. Jing Q, Huang S, Guth S, et al. Involvement of MicroRNA in AU-Rich Element-Mediated mRNA Instability. *Cell*. 2005;120(5):623-634. doi:10.1016/j.cell.2004.12.038

78. Reznik B, Clement SL, Lykke-Andersen J. hnRNP F Complexes with tristetraprolin and stimulates ARE-mRNA decay. *PLoS One*. 2014;9(6). doi:10.1371/journal.pone.0100992

79. Emmons J, Townley-Tilson WHD, Deleault KM, et al. Identification of TTP mRNA targets in human dendritic cells reveals TTP as a critical regulator of dendritic cell maturation. *RNA*. 2008;14(5):888-902. doi:10.1261/rna.748408

80. McGuire VA, Rosner D, Ananieva O, et al. Beta Interferon Production Is Regulated by p38 Mitogen-Activated Protein Kinase in Macrophages via both MSK1/2- and Tristetraprolin-Dependent Pathways. *Mol Cell Biol*. 2017;37(1). doi:10.1128/mcb.00454-16

81. Pfeiffer JR, Brooks SA. Cullin 4B Is Recruited to Tristetraprolin-Containing Messenger Ribonucleoproteins and Regulates TNF-α mRNA Polysome Loading. *J Immunol*. 2012;188(4):1828-1839. doi:10.4049/jimmunol.1102837

82. Taylor GA, Carballo E, Lee DM, et al. A pathogenetic role for TNFα in the syndrome of cachexia, arthritis, and autoimmunity resulting from tristetraprolin (TTP) deficiency. *Immunity*. 1996;4(5):445-454. doi:10.1016/S1074-7613(00)80411-2

83. Qi M-Y, Wang Z-Z, Zhang Z, et al. AU-Rich-Element-Dependent Translation Repression Requires the Cooperation of Tristetraprolin and RCK/P54. *Mol Cell Biol*. 2012;32(5):913-928. doi:10.1128/mcb.05340-11

84. Fenger-Grøn M, Fillman C, Norrild B, Lykke-Andersen J. Multiple processing body factors and the ARE binding protein TTP activate mRNA decapping. *Mol Cell*. 2005;20(6):905-915. doi:10.1016/j.molcel.2005.10.031

85. Clark AR, Dean JLE. The control of inflammation via the phosphorylation and dephosphorylation of tristetraprolin: A tale of two phosphatases. *Biochem Soc Trans*. 2016;44(5):1321-1337. doi:10.1042/BST20160166

86. Cao H, Dzineku F, Blackshear PJ. Expression and purification of recombinant tristetraprolin that can bind to tumor necrosis factor-α mRNA and serve as a substrate for mitogen-activated protein kinases. *Arch Biochem Biophys*. 2003;412(1):106-120. doi:10.1016/S0003-9861(03)00012-2

87. Ngoc L V., Wauquier C, Soin R, et al. Rapid Proteasomal Degradation of Posttranscriptional Regulators of the TIS11/Tristetraprolin Family Is Induced by an Intrinsically Unstructured Region Independently of Ubiquitination. *Mol Cell Biol*. 2014;34(23):4315-4328. doi:10.1128/mcb.00643-14

88. Brook M, Tchen CR, Santalucia T, et al. Posttranslational Regulation of Tristetraprolin Subcellular Localization and Protein Stability by p38 Mitogen-Activated Protein Kinase and Extracellular Signal-Regulated Kinase Pathways. *Mol Cell Biol*. 2006;26(6):2408-2418. doi:10.1128/mcb.26.6.2408-2418.2006

89. Ross EA, Smallie T, Ding Q, et al. Dominant Suppression of Inflammation via Targeted Mutation of the mRNA Destabilizing Protein Tristetraprolin. *J Immunol*. 2015;195(1):265-276. doi:10.4049/jimmunol.1402826

90. Chrestensen CA, Schroeder MJ, Shabanowitz J, et al. MAPKAP Kinase 2 Phosphorylates Tristetraprolin on in Vivo Sites Including Ser178, a Site Required for 14-3-3 Binding. *J Biol Chem*. 2004;279(11):10176-10184.

doi:10.1074/jbc.M310486200

91. Stoecklin G, Stubbs T, Kedersha N, et al. MK2-induced tristetraprolin:14-3-3 Complexes prevent stress granule association and ARE-mRNA decay. *EMBO J*. 2004;23(6):1313-1324. doi:10.1038/sj.emboj.7600163

92. Sun L, Stoecklin G, Van Way S, et al. Tristetraprolin (TTP)-14-3-3 complex formation protects TTP from dephosphorylation by protein phosphatase 2a and stabilizes tumor necrosis factor-α mRNA. *J Biol Chem*. 2007;282(6):3766-3777. doi:10.1074/jbc.M607347200

93. Tiedje C, Diaz-Muñoz MD, Trulley P, et al. The RNA-binding protein TTP is a global post-transcriptional regulator of feedback control in inflammation. *Nucleic Acids Res*. 2016;44(15):7418-7440. doi:10.1093/nar/gkw474

94. Clement SL, Scheckel C, Stoecklin G, Lykke-Andersen J. Phosphorylation of Tristetraprolin by MK2 Impairs AU-Rich Element mRNA Decay by Preventing Deadenylase Recruitment. *Mol Cell Biol*. 2011;31(2):256-266. doi:10.1128/mcb.00717-10

95. Sandler H, Kreth J, Timmers HTM, Stoecklin G. Not1 mediates recruitment of the deadenylase Caf1 to mRNAs targeted for degradation by tristetraprolin. *Nucleic Acids Res*. 2011;39(10):4373-4386. doi:10.1093/nar/gkr011

96. Lykke-Andersen J, Wagner E. Recruitment and activation of mRNA decay enzymes by two ARE-mediated decay activation domains in the proteins TTP and BRF-1. *Genes Dev*. 2005;19(3):351-361. doi:10.1101/gad.1282305

97. Greischel A, Zahn G. Pharmacokinetics of recombinant huan tumor necrosis factor alpha in rhesus monkeys after intravenous administration. *J Pharmacol Exp Ther*. 1989;251(1):358-361.

98. Database for mRNA Half-Life of 19 977 Genes Obtained by DNA Microarray Analysis of Pluripotent and Differentiating Mouse Embryonic Stem Cells - PubMed. https://pubmed.ncbi.nlm.nih.gov/19001483/. Accessed May 2, 2020.

99. Carballo E, Lai WS, Blackshear PJ. Evidence that tristetraprolin is a physiological regulator of granulocyte-macrophage colony-stimulating factor messenger RNA deadenylation and stability. *Blood*. 2000;95(6):1891-1899. doi:10.1182/blood.v95.6.1891

100. Stoecklin G, Tenenbaum SA, Mayo T, et al. Genome-wide analysis identifies interleukin-10 mRNA as target of tristetraprolin. *J Biol Chem*. 2008;283(17):11689-11699. doi:10.1074/jbc.M709657200

101. Kratochvill F, Machacek C, Vogl C, et al. Tristetraprolin-driven regulatory circuit controls quality and timing of mRNA decay in inflammation. *Mol Syst Biol*. 2011;7(1). doi:10.1038/msb.2011.93

102. Chen YL, Huang YL, Lin NY, Chen HC, Chiu WC, Chang CJ. Differential regulation of ARE-mediated TNFα and IL-1β mRNA stability by lipopolysaccharide in RAW264.7 cells. *Biochem Biophys Res Commun*. 2006;346(1):160-168. doi:10.1016/j.bbrc.2006.05.093

103. Ogilvie RL, Abelson M, Hau HH, Vlasova I, Blackshear PJ, Bohjanen PR. Tristetraprolin Down-Regulates IL-2 Gene Expression through AU-Rich Element-Mediated mRNA Decay . *J Immunol*. 2005;174(2):953-961. doi:10.4049/jimmunol.174.2.953

104. Liang J, Lei T, Song Y, Yanes N, Qi Y, Fu M. RNA-destabilizing factor tristetraprolin negatively regulates NF-κB signaling. *J Biol Chem*. 2009;284(43):29383-29390. doi:10.1074/jbc.M109.024745

105. Haneklaus M, O'Neil JD, Clark AR, Masters SL, O'Neill LAJ. The RNA-binding protein Tristetraprolin (TTP) is a critical negative regulator of the NLRP3 inflammasome. *J Biol Chem*. 2017;292(17):6869-6881. doi:10.1074/jbc.M116.772947

106. Kovarik P, Ebner F, Sedlyarov V. Posttranscriptional regulation of cytokine expression. *Cytokine*. 2017;89:21-26. doi:10.1016/j.cyto.2015.11.007

107. Sauer I, Schaljo B, Vogl C, et al. Interferons limit inflammatory responses by induction of tristetraprolin. *Blood*. 2006;107(12):4790-4797. doi:10.1182/blood-2005-07-3058

108. Joe Y, Chen Y, Park J, et al. Cross-talk between CD38 and TTP Is Essential for Resolution of Inflammation during Microbial Sepsis. *Cell Rep*. 2020;30(4):1063-1076.e5. doi:10.1016/j.celrep.2019.12.090

109. Joe Y, Kim SK, Chen Y, et al. Tristetraprolin mediates anti-inflammatory effects of carbon monoxide on lipopolysaccharide-induced acute lung injury. *Am J Pathol*. 2015;185(11):2867-2874. doi:10.1016/j.ajpath.2015.07.002

110. Carballo E. Feedback Inhibition of Macrophage Tumor Necrosis Factor- Production by Tristetraprolin. *Science (80-)*. 1998;281(5379):1001-1005. doi:10.1126/science.281.5379.1001

111. Molle C, Zhang T, De Lendonck LY, et al. Tristetraprolin regulation of interleukin 23 mRNA stability prevents a spontaneous inflammatory disease. *J Exp Med*. 2013;210(9):1675-1684. doi:10.1084/jem.20120707

112. Sneezum L, Eislmayr K, Dworak H, et al. Context-Dependent IL-1 mRNA-Destabilization by TTP Prevents

Dysregulation of Immune Homeostasis Under Steady State Conditions. *Front Immunol*. 2020;11:1398. doi:10.3389/fimmu.2020.01398

113. Andrianne M, Assabban A, La C, et al. Tristetraprolin expression by keratinocytes controls local and systemic inflammation. *JCI insight*. 2017;2(11). doi:10.1172/jci.insight.92979

114. Qiu L-Q, Stumpo DJ, Blackshear PJ. Myeloid-Specific Tristetraprolin Deficiency in Mice Results in Extreme Lipopolysaccharide Sensitivity in an Otherwise Minimal Phenotype. *J Immunol*. 2012;188(10):5150-5159. doi:10.4049/jimmunol.1103700

115. Carballo E, Gilkeson GS, Blackshear PJ. Bone marrow transplantation reproduces the tristetraprolin-deficiency syndrome in recombination activating gene-2 (-/-) mice. Evidence that monocyte/macrophage progenitors may be responsible for TNFα overproduction. *J Clin Invest*. 1997;100(5):986-995. doi:10.1172/JCI119649

116. Grivennikov SI, Tumanov A V., Liepinsh DJ, et al. Distinct and nonredundant in vivo functions of TNF produced by T cells and macrophages/neutrophils: Protective and deleterious effects. *Immunity*. 2005;22(1):93-104. doi:10.1016/j.immuni.2004.11.016

117. Fan Q, Yee CL, Ohyama M, et al. Bone marrow-derived keratinocytes are not detected in normal skin and only rarely detected in wounded skin in two different murine models. *Exp Hematol*. 2006;34(5):672-679. doi:10.1016/j.exphem.2006.02.002

118. Brittan M, Braun KM, Reynolds LE, et al. Bone marrow cells engraft within the epidermis and proliferate in vivo with no evidence of cell fusion. *J Pathol*. 2005;205(1):1-13. doi:10.1002/path.1682

119. Patial S, Blackshear PJ. Tristetraprolin as a Therapeutic Target in Inflammatory Disease. *Trends Pharmacol Sci*. 2016;37(10):811-821. doi:10.1016/j.tips.2016.07.002

120. Patial S, Curtis AD, Lai WS, et al. Enhanced stability of tristetraprolin mRNA protects mice against immune-mediated inflammatory pathologies. *Proc Natl Acad Sci U S A*. 2016;113(7):1865-1870. doi:10.1073/pnas.1519906113

121. Guo J, Qu H, Shan T, Chen Y, Chen Y, Xia J. Tristetraprolin overexpression in gastric cancer cells suppresses PD-L1 expression and inhibits tumor progression by enhancing antitumor immunity. *Mol Cells*. 2018;41(7):653-664. doi:10.14348/molcells.2018.0040

122. Halvorsen EC, Franks SE, Wadsworth BJ, et al. IL-33 increases ST2 + Tregs and promotes metastatic tumour growth in the lungs in an amphiregulin-dependent manner. *Oncoimmunology*. 2019;8(2). doi:10.1080/2162402X.2018.1527497

123. Eshelman MA, Matthews SM, Schleicher EM, et al. Tristetraprolin targets Nos2 expression in the colonic epithelium. *Sci Rep*. 2019;9(1). doi:10.1038/s41598-019-50957-9

124. Parnas O, Jovanovic M, Eisenhaure TM, et al. A Genome-wide CRISPR Screen in Primary Immune Cells to Dissect Regulatory Networks. *Cell*. 2015;162(3):675-686. doi:10.1016/j.cell.2015.06.059

125. Ebner F, Sedlyarov V, Tasciyan S, et al. The RNA-binding protein tristetraprolin schedules apoptosis of pathogen-engaged neutrophils during bacterial infection. *J Clin Invest*. 2017;127(6):2051-2065. doi:10.1172/JCI80631

126. Ivin M. Modulation of the innate immune response during Klebsiella pneumoniae-induced and pneumococcal pneumonia [Unpublished doctoral dissertation], University of Vienna, 2018.

127. Sneezum L. Context dependent regulation of immune homeostasis by TTP [Unpublished doctoral dissertation], University of Vienna, 2020.

128. Schneider DS, Ayres JS. Two ways to survive infection: what resistance and tolerance can teach us about treating infectious diseases. *Nat Rev Immunol*. 2008;8(11):889-895. doi:10.1038/nri2432

129. Kovarik P, Castiglia V, Ivin M, Ebner F. Type I interferons in bacterial infections: A balancing act. *Front Immunol*. 2016;7(DEC):652. doi:10.3389/fimmu.2016.00652

130. Råberg L, Sim D, Read AF. Disentangling genetic variation for resistance and tolerance to infectious diseases in animals. *Science (80-)*. 2007;318(5851):812-814. doi:10.1126/science.1148526

131. Ma Y, Seiler KP, Eichwald EJ, Weis JH, Teuscher C, Weis JJ. Distinct characteristics of resistance to Borrelia burgdorferi induced arthritis in C57BL/6N mice. *Infect Immun*. 1998;66(1):161-168. doi:10.1128/iai.66.1.161-168.1998

132. Gaba A, Grivennikov SI, Do MV, Stumpo DJ, Blackshear PJ, Karin M. Cutting Edge: IL-10–Mediated Tristetraprolin Induction Is Part of a Feedback Loop That Controls Macrophage STAT3 Activation and Cytokine Production. *J Immunol*. 2012;189(5):2089-2093. doi:10.4049/jimmunol.1201126

133. Schaljo B, Kratochvill F, Gratz N, et al. Tristetraprolin Is Required for Full Anti-Inflammatory Response of Murine Macrophages to IL-10. *J Immunol*. 2009;183(2):1197-1206. doi:10.4049/jimmunol.0803883

134. Borroni M. [Unpublished doctoral dissertation in progress], University of Vienna, 2020.

135. Brown CL, Meise KS, Plowman GD, Coffey RJ, Dempsey PJ. Cell surface ectodomain cleavage of human amphiregulin precursor is sensitive to a metalloprotease inhibitor: Release of a predominant N- glycosylated 43-kDa soluble form. *J Biol Chem*. 1998;273(27):17258-17268. doi:10.1074/jbc.273.27.17258

136. Jones JT, Akita RW, Sliwkowski MX. Binding specificities and affinities of egf domains for ErbB receptors. *FEBS Lett*. 1999;447(2-3):227-231. doi:10.1016/S0014-5793(99)00283-5

137. Macdonald-Obermann JL, Pike LJ. Different epidermal growth factor (EGF) receptor ligands show distinct kinetics and biased or partial agonism for homodimer and heterodimer formation. *J Biol Chem*. 2014;289(38):26178-26188. doi:10.1074/jbc.M114.586826

138. Stern KA, Place TL, Lill NL. EGF and amphiregulin differentially regulate Cbl recruitment to endosomes and EGF receptor fate. *Biochem J*. 2008;410(3):585-594. doi:10.1042/BJ20071505

139. Avraham R, Yarden Y. Feedback regulation of EGFR signalling: Decision making by early and delayed loops. *Nat Rev Mol Cell Biol*. 2011;12(2):104-117. doi:10.1038/nrm3048

140. Marshall CJ. Specificity of receptor tyrosine kinase signaling: Transient versus sustained extracellular signal-regulated kinase activation. *Cell*. 1995;80(2):179-185. doi:10.1016/0092-8674(95)90401-8

141. Kimura H, Schubert D. Schwannoma-derived growth factor promotes the neuronal differentiation and survival of PC12 cells. *J Cell Biol*. 1992;116(3):777-783. doi:10.1083/jcb.116.3.777

142. Chung E, Graves-Deal R, Franklin JL, Coffey RJ. Differential effects of amphiregulin and TGF-α on the morphology of MDCK cells. *Exp Cell Res*. 2005;309(1):149-160. doi:10.1016/j.yexcr.2005.05.012

143. Mukhopadhyay C, Zhao X, Maroni D, Band V, Naramura M. Distinct Effects of EGFR Ligands on Human Mammary Epithelial Cell Differentiation. *PLoS One*. 2013;8(10). doi:10.1371/journal.pone.0075907

144. Pasic L, Karin Eisinger-Mathason TS, Velayudhan BT, et al. Sustained activation of the HER1-ERK1/2-RSK signaling pathway controls myoepithelial cell fate in human mammary tissue. *Genes Dev*. 2011;25(15):1641-1653. doi:10.1101/gad.2025611

145. Latasa MU, Salis F, Urtasun R, et al. Regulation of Amphiregulin Gene Expression by β-Catenin Signaling in Human Hepatocellular Carcinoma Cells: A Novel Crosstalk between FGF19 and the EGFR System. *PLoS One*. 2012;7(12). doi:10.1371/journal.pone.0052711

146. Koeppen M, Lee JW, Seo SW, et al. Hypoxia-inducible factor 2-alpha-dependent induction of amphiregulin dampens myocardial ischemia-reperfusion injury. *Nat Commun*. 2018;9(1). doi:10.1038/s41467-018-03105-2

147. Lee SB, Huang K, Palmer R, et al. The Wilms tumor suppressor WT1 encodes a transcriptional activator of amphiregulin. *Cell*. 1999;98(5):663-673. doi:10.1016/S0092-8674(00)80053-7

148. Berasain C, García-Trevijano ER, Castillo J, et al. Amphiregulin: An early trigger of liver regeneration in mice. *Gastroenterology*. 2005;128(2):424-432. doi:10.1053/j.gastro.2004.11.006

149. Busser B, Sancey L, Brambilla E, Coll JL, Hurbin A. The multiple roles of amphiregulin in human cancer. *Biochim Biophys Acta - Rev Cancer*. 2011;1816(2):119-131. doi:10.1016/j.bbcan.2011.05.003

150. Stoll SW, Stuart PE, Lambert S, et al. Membrane-Tethered Intracellular Domain of Amphiregulin Promotes Keratinocyte Proliferation. *J Invest Dermatol*. 2016;136(2):444-452. doi:10.1016/j.jid.2015.10.061

151. Stoll SW, Stuart PE, Swindell WR, et al. The EGF receptor ligand amphiregulin controls cell division via FoxM1. *Oncogene*. 2016;35(16):2075-2086. doi:10.1038/onc.2015.269

152. Goda C, Balli D, Black M, et al. Loss of FOXM1 in macrophages promotes pulmonary fibrosis by activating p38 MAPK signaling pathway. Barsh GS, ed. *PLOS Genet*. 2020;16(4):e1008692. doi:10.1371/journal.pgen.1008692

153. Minutti CM, Modak R V., Macdonald F, et al. A Macrophage-Pericyte Axis Directs Tissue Restoration via Amphiregulin-Induced Transforming Growth Factor Beta Activation. *Immunity*. 2019;50(3):645-654.e6. doi:10.1016/j.immuni.2019.01.008

154. Bennett KL, Plowman GD, Buckley SD, Skonier J, Purchio AF. Regulation of amphiregulin mRNA by TGF-β in the human lung adenocarcinoma cell line a549. *Growth Factors*. 1992;7(3):207-213. doi:10.3109/08977199209046925

155. Burzyn D, Kuswanto W, Kolodin D, et al. A Special Population of regulatory T Cells Potentiates muscle repair. *Cell*. 2013;155(6):1282-1295. doi:10.1016/j.cell.2013.10.054

156. Ogata-Suetsugu S, Yanagihara T, Hamada N, et al. Amphiregulin suppresses epithelial cell apoptosis in lipopolysaccharide-induced lung injury in mice. *Biochem Biophys Res Commun*. 2017;484(2):422-428. doi:10.1016/j.bbrc.2017.01.142

157. Monticelli LA, Sonnenberg GF, Abt MC, et al. Innate lymphoid cells promote lung-tissue homeostasis after infection with influenza virus. *Nat Immunol*. 2011;12(11):1045-1054. doi:10.1038/ni.2131

158. Poole JA, Nordgren TM, Heires AJ, et al. Amphiregulin modulates murine lung recovery and fibroblast function following exposure to agriculture organic dust. *Am J Physiol Cell Mol Physiol*. November 2019:ajplung.00039.2019. doi:10.1152/ajplung.00039.2019

159. Okoye IS, Coomes SM, Pelly VS, et al. MicroRNA-Containing T-Regulatory-Cell-Derived Exosomes Suppress Pathogenic T Helper 1 Cells. *Immunity*. 2014;41(1):89-103. doi:10.1016/j.immuni.2014.05.019

160. Zaiss DMW, van Loosdregt J, Gorlani A, et al. Amphiregulin Enhances Regulatory T Cell-Suppressive Function via the Epidermal Growth Factor Receptor. *Immunity*. 2013;38(2):275-284. doi:10.1016/j.immuni.2012.09.023

161. Luetteke NC, Qiu TH, Fenton SE, et al. Targeted inactivation of the EGF and amphiregulin genes reveals distinct roles for EGF receptor ligands in mouse mammary gland development. *Development*. 1999;126(12):2739-2750. https://pubmed.ncbi.nlm.nih.gov/10331984/. Accessed May 2, 2020.

162. Zaiss DMW, Gause WC, Osborne LC, Artis D. Emerging functions of amphiregulin in orchestrating immunity, inflammation and tissue repair. *Immunity*. 2015;42(2):216. doi:10.1016/J.IMMUNI.2015.01.020

163. Pulendran B, Artis D. New paradigms in type 2 immunity. *Science (80-)*. 2012;337(6093):431-435. doi:10.1126/science.1221064

164. Allen JE, Wynn TA. Evolution of Th2 Immunity: A Rapid Repair Response to Tissue Destructive Pathogens. *PLoS Pathog*. 2011;7(5). doi:10.1371/journal.ppat.1002003

165. Zaiss DM, Yang L, Shah PR, Kobie JJ, Urban JF, Mosmann TR. Amphiregulin, a TH2 cytokine enhancing resistance to nematodes. *Science (80-)*. 2006;314(5806):1746. doi:10.1126/science.1133715

166. Flannagan RS, Jaumouillé V, Grinstein S. The Cell Biology of Phagocytosis. *Annu Rev Pathol Mech Dis*. 2012;7(1):61-98. doi:10.1146/annurev-pathol-011811-132445

167. Pålsson-McDermott EM, O'Neill LAJ. Signal transduction by the lipopolysaccharide receptor, Toll-like receptor-4. *Immunology*. 2004;113(2):153-162. doi:10.1111/j.1365-2567.2004.01976.x

168. Moretti J, Blander JM. Insights into phagocytosis-coupled activation of pattern recognition receptors and inflammasomes. *Curr Opin Immunol*. 2014;26(1):100-110. doi:10.1016/j.coi.2013.11.003

169. van der Laan LJ, Döpp EA, Haworth R, et al. Regulation and functional involvement of macrophage scavenger receptor MARCO in clearance of bacteria in vivo. *J Immunol*. 1999;162(2):939-947. https://pubmed.ncbi.nlm.nih.gov/9916718/. Accessed July 27, 2020.

170. Sulahian TH, Imrich A, DeLoid G, Winkler AR, Kobzik L. Signaling pathways required for macrophage scavenger receptor-mediated phagocytosis: Analysis by scanning cytometry. *Respir Res*. 2008;9(1):59. doi:10.1186/1465-9921-9-59

171. Botelho RJ, Teruel M, Dierckman R, et al. Localized biphasic changes in phosphatidylinositol-4,5-bisphosphate at sites of phagocytosis. *J Cell Biol*. 2000;151(7):1353-1367. doi:10.1083/jcb.151.7.1353

172. Sedlyarov V, Eichner R, Girardi E, et al. The Bicarbonate Transporter SLC4A7 Plays a Key Role in Macrophage Phagosome Acidification. *Cell Host Microbe*. 2018;23(6):766-774.e5. doi:10.1016/j.chom.2018.04.013

173. Mukherjee N, Jacobs NC, Hafner M, et al. Global target mRNA specification and regulation by the RNA-binding protein ZFP36. *Genome Biol*. 2014;15(1):R12. doi:10.1186/gb-2014-15-1-r12

174. Ostuni R, Piccolo V, Barozzi I, et al. Latent enhancers activated by stimulation in differentiated cells. *Cell*. 2013;152(1-2):157-171. doi:10.1016/j.cell.2012.12.018

175. Pham LN, Dionne MS, Shirasu-Hiza M, Schneider DS. A specific primed immune response in Drosophila is dependent on phagocytes. *PLoS Pathog*. 2007;3(3). doi:10.1371/journal.ppat.0030026

176. Geigges M, Arekatla G, Paro R. Priming exposures to lipopolysaccharides do not affect the induction of Polycomb target genes upon re-exposure. *PLoS One*. 2020;15(4). doi:10.1371/journal.pone.0231498

177. Lamprou I, Mamali I, Dallas K, Fertakis V, Lampropoulou M, Marmaras VJ. Distinct signalling pathways promote phagocytosis of bacteria, latex beads and lipopolysaccharide in medfly haemocytes. *Immunology*. 2007;121(3):314-327. doi:10.1111/j.1365-2567.2007.02576.x

178. Miles AA, Misra SS, Irwin JO. The estimation of the bactericidal power of the blood. *J Hyg (Lond)*. 1938;38(6):732-749. doi:10.1017/S002217240001158X

8 Supplementary Material – German summary

Für die Aufrechterhaltung eines gesunden Körperzustandes ist eine strenge Regulation des Immunsystems erforderlich. Dabei ist Tristetraprolin (TTP) ein wichtiger Faktor, da es die mRNA von Zytokinen und Chemokinen destabilisiert, wodurch es zum Abklingen der Entzündung und zur Wiederherstellung der Immunhomöostase kommt.

Vorangehende Experimente haben gezeigt, dass Mäuse, denen TTP in ihrer myeloiden Zelllinie fehlt, Infektionen mit *Streptococcus pneumoniae* besser überleben können und reduzierte Entzündungsreaktionen zeigen. Um die Rolle von TTP in diesem Infektionsmodel zu untersuchen, verfolgten wir zwei unterschiedliche Hypothesen.

Einerseits könnte die verbesserte Überlebenschance an verstärkter Toleranz gegenüber pathogenverursachten Gewebeschäden liegen. Als Vertreter der Toleranzfaktoren wurde Amphiregulin (Areg), ein EGF Rezeptor Ligand, welcher mit Zelldifferenzierung, -proliferation und Wundheilung in Verbindung gebracht wird, daraufhin getestet, ob TTP dessen mRNA bindet und destabilisiert. Ein Reporterkonstrukt, das Aregs 3‘ untranslatierte Region hinter einem Luziferase-Gen beinhaltet, wurde in mRNA Stabilitätstests und Immunpräzipitationsexperimenten eingesetzt, doch es konnte nicht gezeigt werden, ob TTP an Areg mRNA bindet, da die experimentelle Methode nicht ausreichend optimiert werden konnte.

Andererseits könnte eine erhöhte Resistenz gegen das Pathogen, ausgedrückt durch eine effektivere Eliminierung der Bakterien, den beobachteten Phänotyp erklären. Daher wurde die Phagozytose verschiedener Bakterien und Latexperlen durch unterschiedliche Makrophagenarten untersucht. Dies zeigte, dass TTP Phagozytoseaktivität verringert. Während TTP anscheinend keine Rolle beim Beseitigen von bereits aufgenommenen Bakterien spielt, könnte die gesteigerte Partikelaufnahme der Grund für die erfolgreichere Immunantwort in infizierten Mäusen ohne myeloides TTP sein.

Diese Studie erweitert die Auffassung von TTP und zeigt das Protein als einen antiinflammatorischen Faktor, der auch am Mechanismus der Phagozytose beteiligt ist.